JEM Journal of Experimental Medicine

ARTICLE

β-Catenin induces transcriptional expression of PD-L1 to promote glioblastoma immune evasion

Linyong Du[1,2*], Jong-Ho Lee[3*], Hongfei Jiang[4], Chengde Wang[5], Silu Wang[6], Zhihong Zheng[7], Fei Shao[4], Daqian Xu[8], Yan Xia[2], Jing Li[9], Yanhua Zheng[2], Xu Qian[10,11], Xinjian Li[12], Hyung-Ryong Kim[13], Dongming Xing[4,14], Pengyuan Liu[7], Zhimin Lu[8], and Jianxin Lyu[1,15]

PD-L1 up-regulation in cancer contributes to immune evasion by tumor cells. Here, we show that Wnt ligand and activated EGFR induce the binding of the β-catenin/TCF/LEF complex to the *CD274* gene promoter region to induce PD-L1 expression, in which AKT activation plays an important role. β-Catenin depletion, AKT inhibition, or PTEN expression reduces PD-L1 expression in tumor cells, enhances activation and tumor infiltration of CD8⁺ T cells, and reduces tumor growth, accompanied by prolonged mouse survival. Combined treatment with a clinically available AKT inhibitor and an anti–PD-1 antibody overcomes tumor immune evasion and greatly inhibits tumor growth. In addition, AKT-mediated β-catenin S552 phosphorylation and nuclear β-catenin are positively correlated with PD-L1 expression and inversely correlated with the tumor infiltration of CD8⁺ T cells in human glioblastoma specimens, highlighting the clinical significance of β-catenin activation in tumor immune evasion.

Introduction

The interaction between programmed cell death 1 (PD-1) on T cells and programmed cell death ligand 1 (PD-L1; also known as B7-H1) on tumor cells inhibits the activation, expansion, and effector functions of antigen-specific CD8⁺ T cells and promotes T cell apoptosis and the induction of regulatory T cells (T reg or suppressor T cells), allowing cancer cells to evade immune destruction (Boussiotis, 2016; Sharma et al., 2017).

Therapeutic targeting of immune checkpoints has resulted in tumor regression in melanoma and non–small cell lung cancer, and clinical trials are ongoing in glioblastoma (GBM) and several other types of cancer (Sharma and Allison, 2015). However, only a portion of patients experience a response to this immunotherapy (Sharma and Allison, 2015). The response to PD-1/PD-L1 blockade is reported to be correlated with PD-L1 expression levels in tumor cells (Herbst et al., 2014; Iwai et al., 2002). Although it has been reported that PD-L1 expression can be up-regulated at transcriptional (Casey et al., 2016; Dorand et al., 2016), translational (Coelho et al., 2017; Parsa et al., 2007), and posttranslational levels via inhibition of its protein ubiquitylation (Li et al., 2016; Lim et al., 2016; Zhang et al., 2018), it remains unclear whether the tumor microenvironment that activates growth factor receptor plays a role in the regulation of PD-L1 transcription and tumor immune evasion.

Aberrant activation of Wnt/β-catenin signaling has been detected in various types of cancer, such as breast, prostate, lung, and hematopoietic malignancies and GBM, and nuclear

[1]Key Laboratory of Laboratory Medicine, Ministry of Education of China, School of Laboratory Medicine and Life Science, Wenzhou Medical University, Wenzhou, Zhejiang, China; [2]Brain Tumor Center and Department of Neuro-Oncology, The University of Texas MD Anderson Cancer Center, Houston, TX; [3]Department of Biological Sciences, Dong-A University, Busan, Republic of Korea; [4]The Affiliated Hospital of Qingdao University, Qingdao Cancer Institute, Qingdao, Shandong, China; [5]Department of Neurosurgery, First Affiliated Hospital of Wenzhou Medical University, Wenzhou Medical University, Wenzhou, Zhejiang, China; [6]Key Laboratory of Diagnosis and Treatment of Severe Hepato-Pancreatic Diseases of Zhejiang Province, The First Affiliated Hospital of Wenzhou Medical University, Wenzhou Medical University, Wenzhou, Zhejiang, China; [7]Department of Respiratory Medicine, Sir Run Run Shaw Hospital and Institute of Translational Medicine, Zhejiang University School of Medicine, Hangzhou, Zhejiang, China; [8]Department of Hepatobiliary and Pancreatic Surgery and Zhejiang Provincial Key Laboratory of Pancreatic Disease of The First Affiliated Hospital, Institute of Translational Medicine, Zhejiang University School of Medicine, Hangzhou, Zhejiang, China; [9]State Key Laboratory of Oral Diseases, National Clinical Research Center for Oral Diseases, West China Hospital of Stomatology, Sichuan University, Chengdu, Sichuan, China; [10]Department of Nutrition and Food Hygiene, Center for Global Health, School of Public Health, Nanjing Medical University, Nanjing, Jiangsu, China; [11]Institute for Brain Tumors, Jiangsu Key Lab of Cancer Biomarkers, Prevention and Treatment, Jiangsu Collaborative Innovation Center for Cancer Personalized Medicine, Nanjing Medical University, Nanjing, Jiangsu, China; [12]Chinese Academy of Sciences Key Laboratory of Infection and Immunity, Chinese Academy of Sciences Center for Excellence in Biomacromolecules, Institute of Biophysics, Chinese Academy of Sciences, Beijing, China; [13]College of Dentistry, Dankook University, Cheonan, Republic of Korea; [14]School of Life Sciences, Tsinghua University, Beijing, China; [15]People's Hospital of Hangzhou Medical College, Hangzhou, Zhejiang, China.

*L. Du and J.-H. Lee contributed equally to this paper; Correspondence to Jianxin Lyu: jxlu313@163.com; Zhimin Lu: zhiminlu@zju.edu.cn.

accumulation of β-catenin has been shown to be positively correlated with poor clinical outcomes, such as cancer progression, invasion, metastasis, and recurrence, resulting in low survival rates (Anastas and Moon, 2013; Kim et al., 2017; Nusse and Clevers, 2017). The binding of Wnt ligand to the low-density lipoprotein receptor-related protein-5/6 and Frizzled receptors results in the inhibition of GSK-3β–mediated phosphorylation of β-catenin. Stabilized β-catenin migrates to the nucleus, interacting with T cell–specific factor (TCF)/lymphoid enhancer–binding factor (LEF) and coactivators to activate Wnt target gene expression (MacDonald et al., 2009). Notably, Wnt-independent β-catenin transactivation has been implicated in tumor development (Lu and Hunter, 2004). Epidermal growth factor (EGF) receptor (EGFR) activation, resulting from the mutation or overexpression of EGFR in many types of human cancer, activates β-catenin (Ji et al., 2009; Lu et al., 2003; Yang et al., 2011). In addition to stabilizing β-catenin by phosphorylating GSK-3β, AKT, which is activated by growth factor receptors and phosphoinositide 3-kinase (PI3K) activation, phosphatase and tensin homolog (PTEN) mutation, or Wnt3A through mTORC2 activation (Esen et al., 2013), directly phosphorylates β-catenin at Ser552 to release its binding to adherens proteins, thereby promoting the nuclear translocation and activation of β-catenin (Fang et al., 2007; Ji et al., 2009; Lu et al., 2003).

In this study, we demonstrated that β-catenin activation induced by both Wnt ligand and activated EGFR results in the binding of the β-catenin/TCF/LEF complex to the promoter region of the *CD274* gene to induce PD-L1 expression. Inhibition of AKT or β-catenin depletion reduced PD-L1 expression in tumor cells, enhanced $CD8^+$ T cell activation and infiltration into tumors, and reduced tumor growth.

Results

Wnt-induced β-catenin activation results in PD-L1 up-regulation in tumor cells

To determine the relationship between β-catenin activation and immune checkpoints, we performed immunohistochemical (IHC) analyses of tumor tissues from 20 patients with low-grade diffuse astrocytoma (World Health Organization grade II), 20 patients with anaplastic astrocytoma (grade III), and 50 patients with GBM (grade IV). We found that the levels of activated nuclear β-catenin, which were positively correlated with PD-L1 expression levels and glioma grades, were inversely correlated with $CD8^+$ T cell infiltration (Fig. 1 A and Fig. S1 A). Treatment of U251, EGFR-overexpressing U87 (U87/EGFR), and LN18 human GBM cells; glioma stem cell (GSC) 6–27 and GSC 7–11 human primary glioma-initiating cells; CT-2A and GL261 mouse glioma cells; DU145 human prostate cancer cells; and PC14 human lung adenocarcinoma cells with Wnt3A stabilized β-catenin protein and increased PD-L1 expression (Fig. 1 B). Flow cytometry analyses revealed that Wnt3A enhanced the PD-L1 protein expression level on the surface of U87/EGFR cells (Fig. 1 C).

Pretreatment of GBM cells with actinomycin D, a transcription inhibitor, reduced Wnt3A-enhanced PD-L1 expression (Fig. 1 D and Fig. S1 B), suggesting that gene transcription regulation of PD-L1 is involved in the response to Wnt3A treatment. Consistently, quantitative PCR analyses showed that Wnt3A enhanced mRNA levels of the *CD274* gene (encoding PD-L1; Fig. 1 E) without obviously affecting *CD274* mRNA stability (Fig. S1 C) and *Ccl4* chemokine gene expression involved in T cell exclusion (Spranger et al., 2015; Fig. S1 D); this increase, together with the increased protein expression of PD-L1 and β-catenin, was attenuated by β-catenin shRNA expression (Fig. 1 F and Fig. S1 E). In addition, expression of the constitutively active β-catenin (CA β-catenin) mutant (Guo et al., 2012) increased *CD274* mRNA expression (Fig. 1 G, top panel) and PD-L1 total expression (Fig. 1 G, bottom panel) and surface protein expression (Fig. 1 H). These results indicate that Wnt-induced β-catenin activation results in transcriptional up-regulation of PD-L1 in tumor cells.

AKT activation induced by EGFR-dependent PI3K activation, PTEN loss, and Wnt3A enhances PD-L1 expression in a β-catenin–dependent manner

EGFR activation enhances β-catenin activity (Ji et al., 2009; Lu et al., 2003; Yang et al., 2011). As expected, EGF treatment of GBM cells (Fig. 2 A, left panel) or expression of the active EGFRvIII mutant (Fig. 2 A, right panel), which lacks 267 amino acids in its extracellular domain and is commonly found in GBM as well as breast, ovarian, prostate, and lung carcinomas (Kuan et al., 2001; Yang et al., 2012a), increased *CD274* mRNA and PD-L1 protein expression.

Pretreatment of U87/EGFR (Fig. 2 B) and U251 cells (Fig. S2 A) with actinomycin D greatly inhibited EGF-enhanced PD-L1 expression, and depletion of β-catenin reduced *CD274* mRNA and PD-L1 protein expression levels in U87/EGFRvIII cells (Fig. 2 C) and U251 cells treated with EGF (Fig. S2 B). In addition, in the presence of actinomycin D, β-catenin depletion failed to obviously alter *CD274* mRNA levels (Fig. S2 C), suggesting that β-catenin primarily regulates PD-L1 expression through transcriptional regulation of *CD274* mRNA expression.

Notably, reconstituted expression of RNAi-resistant (r) WT β-catenin, but not the rβ-catenin S552A mutant, which is resistant to phosphorylation and activation by AKT (Fang et al., 2007), largely restored the reduced *CD274* mRNA and PD-L1 protein expression in U87/EGFRvIII cells (Fig. 2 D), suggesting that AKT-dependent β-catenin activation is instrumental for EGFR activation-increased PD-L1 expression. Consistent with this result, expression of a constitutively active, myristoylation signal–attached AKT1 (myr-AKT1), which phosphorylates β-catenin at S552, enhanced *CD274* mRNA and PD-L1 expression levels (Fig. 2 E). In contrast, treatment with AKT inhibitor MK2206 or PI3K inhibitor LY294002, which reduced β-catenin S552 phosphorylation, led to reduced *CD274* mRNA and PD-L1 expression levels in U87/EGFRvIII cells (Fig. 2 F) and U251 cells treated with EGF (Fig. S2 D). Similarly, MK2206 treatment inhibited EGF-induced PD-L1 expression in GSC 6–27 and GSC 7–11 cells (Fig. S2 E).

Notably, the inhibitory effect of MK2206 on *CD274* mRNA and PD-L1 protein expression in U87/EGFRvIII cells was abrogated by the expression of CA β-catenin (Fig. 2 G). In addition, overexpression of PTEN, which reduced the phosphorylation levels of AKT T308 and S473 and β-catenin

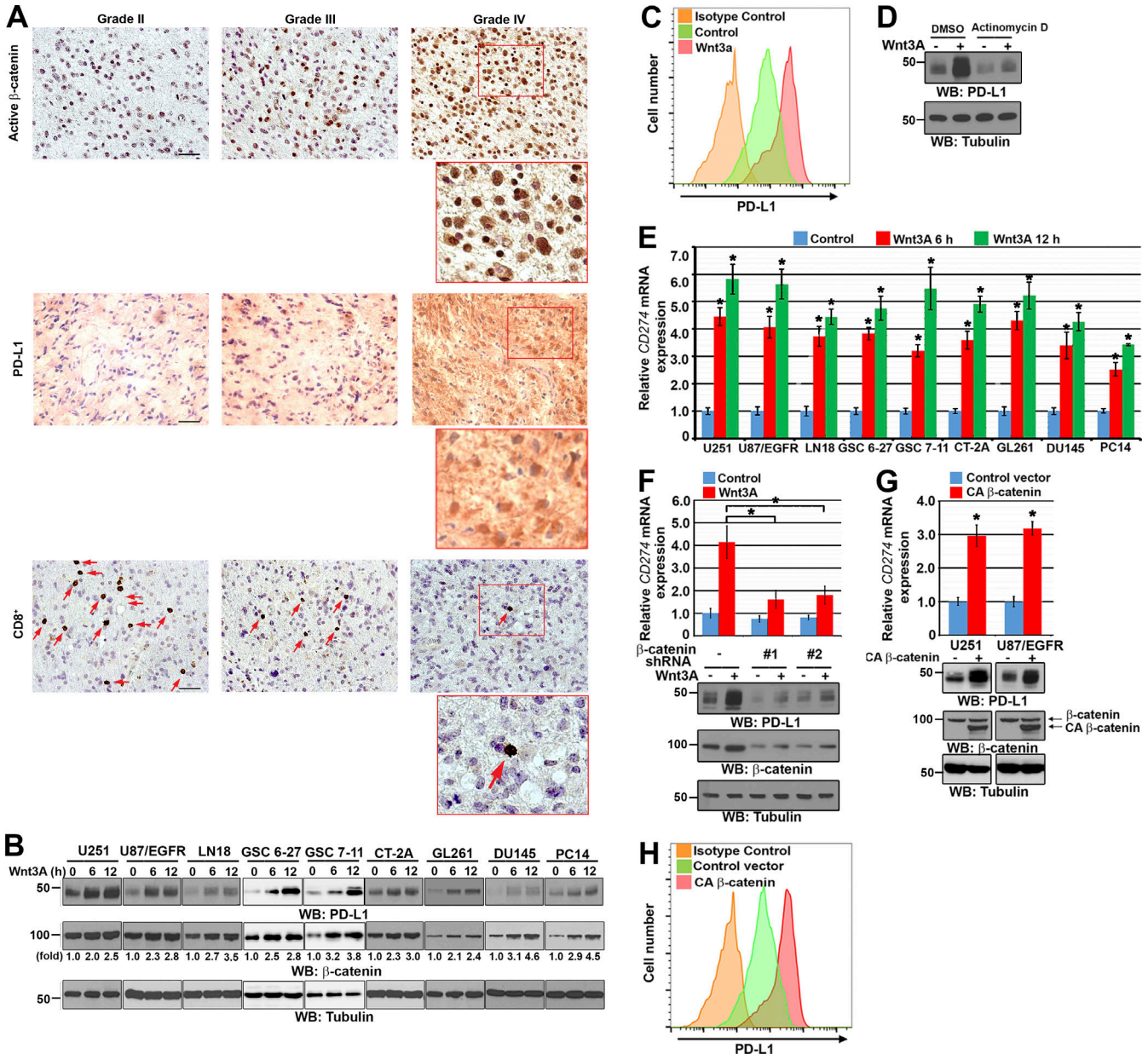

Figure 1. **Wnt-induced β-catenin activation results in PD-L1 up-regulation in tumor cells. (B, D, F, and G)** Immunoblotting analyses were performed with the indicated antibodies. **(E–G)** Data represent the means ± SD of three independent experiments. **(A)** IHC staining of 20 diffuse astrocytoma (grade II), 20 anaplastic astrocytoma (grade III), and 50 GBM (grade IV) specimens was performed with the indicated antibodies. Representative images of IHC staining from the specimens are shown. Scale bar, 50 µm. Red arrows point to $CD8^+$ cells. **(B)** The indicated tumor cells were serum starved for 12 h and then stimulated with Wnt3A (20 ng/ml) for the indicated periods of time. Immunoblotting analyses were performed. **(C)** U87/EGFR cells were treated with or without Wnt3A (20 ng/ml) for 12 h. A cell surface analysis of PD-L1 protein was performed using a flow cytometer. **(D)** Serum-starved U87/EGFR cells were pretreated with or without actinomycin D (1 µg/ml) for 2 h and then stimulated with or without Wnt3A (20 ng/ml) for 12 h. **(E)** The indicated tumor cells were serum starved for 12 h and then stimulated with or without Wnt3A (20 ng/ml) for the indicated periods of time. Real-time PCR analyses were performed. *, $P < 0.0001$, on the basis of Student's *t* test. **(F)** U87/EGFR cells with stable expression of β-catenin shRNA or a control shRNA were treated with or without Wnt3A (20 µg/ml) for 12 h. A real-time PCR analysis (top panel) and immunoblotting analyses (bottom panel) were performed. β-Catenin shRNA#2 was used for the subsequent experiments. *, $P < 0.0001$, on the basis of Student's *t* test. **(G)** U251 and U87/EGFR cells were transfected with control vector or CA β-catenin for 48 h. A real-time PCR analysis (top panel) and immunoblotting analyses (bottom panel) were performed. *, $P < 0.0001$, on the basis of Student's *t* test. **(H)** A control vector or CA β-catenin was stably expressed in U87/EGFR cells. A cell surface analysis of PD-L1 protein was performed using a flow cytometer. WB, Western blot.

S552, reduced *CD274* mRNA and PD-L1 protein expression in EGF-treated PTEN-deficient U251 and U87 cells (Lee et al., 2017; Fig. 2 H). These results indicate that AKT activated by the EGFR-PI3K cascade phosphorylates β-catenin S552 and induces β-catenin–dependent up-regulation of *CD274* transcription and PD-L1 expression in tumor cells.

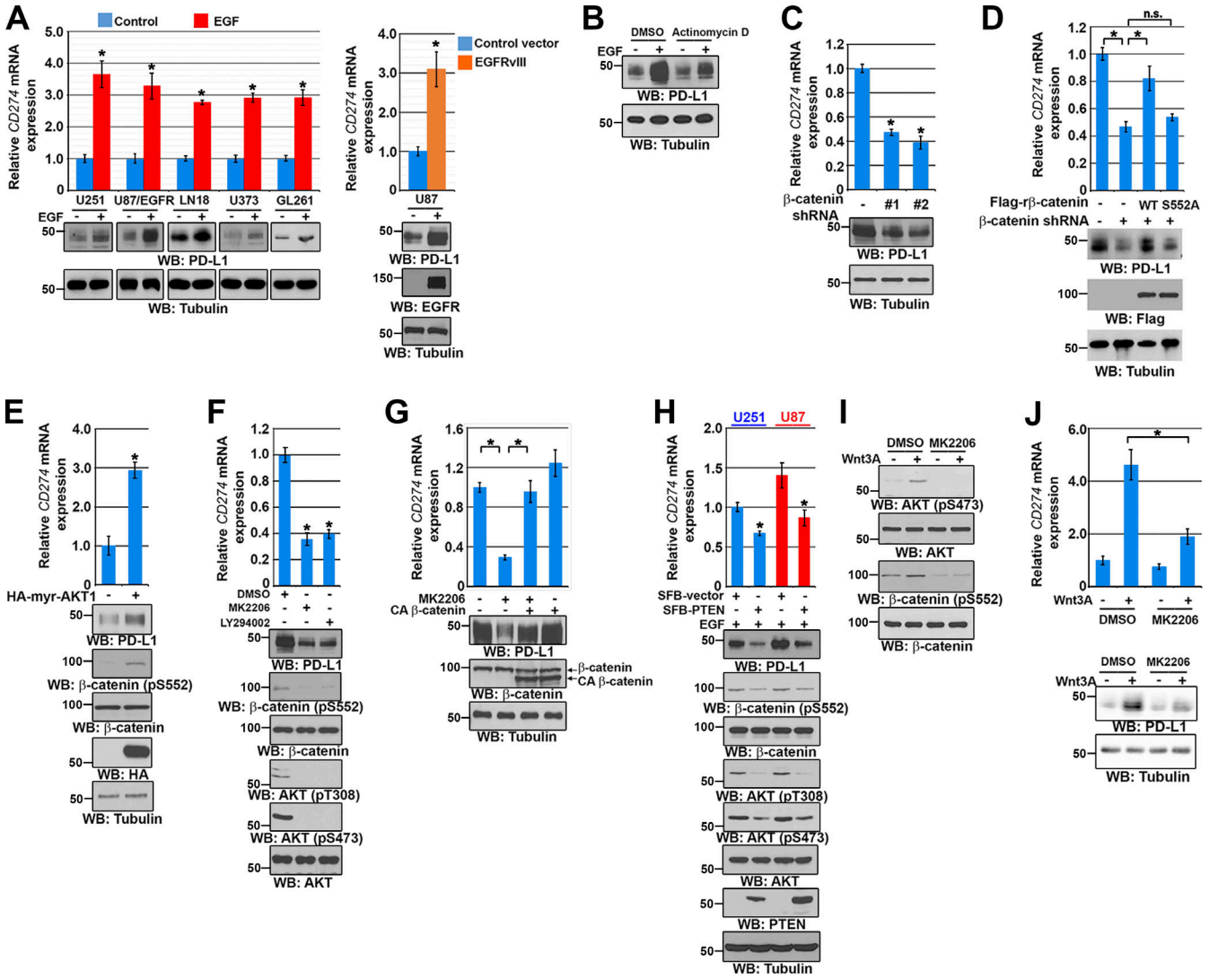

Figure 2. **AKT activation induced by EGFR-dependent PI3K activation, PTEN loss, and Wnt3A enhances PD-L1 expression in a β-catenin–dependent manner. (A–J)** Real-time PCR analyses or immunoblotting analyses were performed with the indicated primer or antibodies. **(A, C–H, J)** Data represent the means ± SD of three independent experiments. **(A)** Left panel: The indicated tumor cells were serum starved for 12 h and then stimulated with or without EGF (100 ng/ml) for 12 h. Right panel: U87 cells were stably transfected with plasmids expressing control vector or EGFRvIII. Real-time PCR analyses (top panel) and immunoblotting analyses (bottom panel) were performed. *, P < 0.0001, on the basis of Student's *t* test. **(B)** Serum-starved U87/EGFR cells were pretreated with or without actinomycin D (1 µg/ml) for 2 h and then stimulated with or without EGF (100 ng/ml) for 12 h. **(C)** U87/EGFRvIII cells were stably expressed with a β-catenin shRNA or a control shRNA. *, P < 0.0001, on the basis of Student's *t* test. **(D)** U87/EGFRvIII cells with stable expression of the β-catenin shRNA or a control shRNA were reconstituted with or without WT rβ-catenin or rβ-catenin S552A mutant. *, P < 0.001, on the basis of the one-way ANOVA; n.s., not significant. **(E)** U87/EGFR cells were stably transfected with an HA vector or HA-myr-AKT1. *, P < 0.0001, on the basis of Student's *t* test. **(F)** Serum-starved U87/EGFRvIII cells were treated with DMSO, MK2206 (5 µM), or LY294002 (20 µM) for 12 h. *, P < 0.0001, on the basis of Student's *t* test. **(G)** U87/EGFRvIII cells were transfected with control vector or CA β-catenin for 48 h and then treated with DMSO or MK2206 (5 µM) for 12 h. *, P < 0.001, on the basis of one-way ANOVA. **(H)** U251 and U87 cells were transfected with SFB-tagged control vector or SFB-PTEN for 48 h and then treated with EGF (100 ng/ml) for 12 h. *, P < 0.001, on the basis of Student's *t* test. **(I)** U87/EGFR cells were pretreated with DMSO or MK2206 (5 µM) for 2 h and then stimulated with or without Wnt3A (20 ng/ml) for 30 min. **(J)** U87/EGFR cells were pretreated with DMSO or MK2206 (5 µM) for 2 h and then stimulated with or without Wnt3A (20 ng/ml) for 12 h. *, P < 0.01, on the basis of Student's *t* test. WB, Western blotting.

AKT can also be activated by Wnt3A through mTORC2 activation (Esen et al., 2013). As expected, MK2206 treatment inhibited Wnt3A-induced AKT S473 phosphorylation, β-catenin S552 phosphorylation, and *CD274* mRNA and PD-L1 expression in U87/EGFR cells (Fig. 2, I and J). These results indicate that AKT activation is also instrumental for Wnt3A-induced and β-catenin activation-mediated up-regulation of *CD274* transcription and PD-L1 protein expression levels in tumor cells. The partial inhibition of Wnt3A-induced *CD274* transcription and PD-L1 protein expression by MK2206 treatment is likely due to AKT-independent and Wnt-direct activation of β-catenin.

The β-catenin/TCF/LEF complex binds to the *CD274* promoter region in response to AKT activation and enhances *CD274* transcription

To identify the binding sequence of TCF/LEF in the promoter region of *CD274*, we analyzed the *CD274* promoter and found that

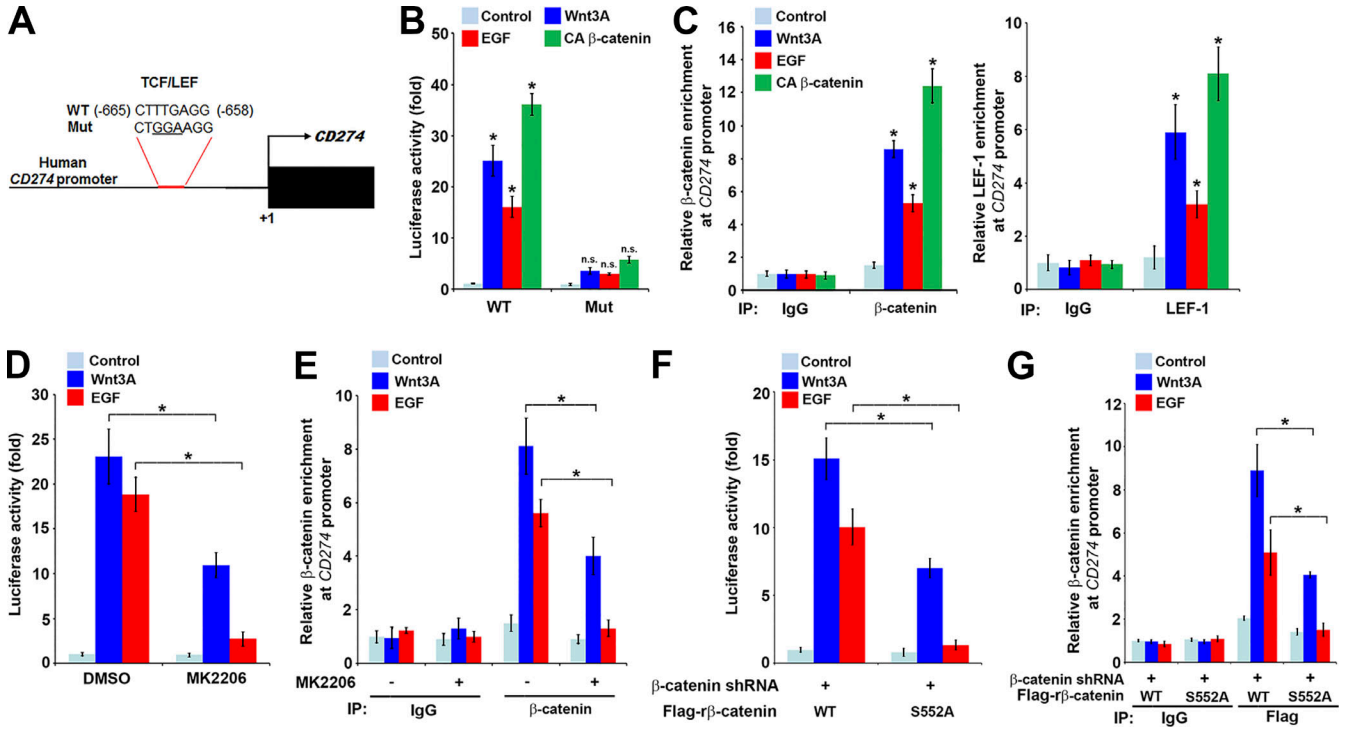

Figure 3. **β-Catenin/TCF/LEF complex binds to the *CD274* promoter region in response to AKT activation and enhances *CD274* transcription. (B–G)** Data represent the means ± SD of three independent experiments. **(A)** Schematic illustration of the proximal region of human *CD274* promoter. **(B)** U87/EGFR cells were transfected with luciferase reporter vectors containing WT or TCF/LEF mutant sequences of *CD274* promoter (600 bp upstream from the transcription start site). After cotransfection with a control vector or a vector expressing CA β-catenin, the cells were stimulated with or without Wnt3A (20 ng/ml) or EGF (100 ng/ml) for 12 h. Luciferase activity was measured. *, P < 0.0001, on the basis of Student's *t* test; n.s., not significant. **(C)** U87/EGFR cells were transfected with a control vector or a vector expressing CA β-catenin for 48 h or stimulated with or without Wnt3A (20 ng/ml) or EGF (100 ng/ml) for 12 h. ChIP assays were performed with an anti-IgG, anti–β-catenin (left panel) or anti-LEF1 antibody (right panel), and quantitative PCR analyses were performed with primers against the promoter of *CD274*. *, P < 0.0001, on the basis of Student's *t* test. **(D)** U87/EGFR cells with expression of a luciferase reporter vector containing WT TCF/LEF sequence of *CD274* promoter were pretreated with or without MK2206 (5 μM) for 2 h and then stimulated with or without Wnt3A (20 ng/ml) or EGF (100 ng/ml) for 12 h. Luciferase activity was measured. *, P < 0.01, on the basis of Student's *t* test. **(E)** U87/EGFR cells were pretreated with or without MK2206 (5 μM) for 2 h and then stimulated with or without Wnt3A (20 ng/ml) or EGF (100 ng/ml) for 12 h. ChIP assays were performed with an anti–IgG or anti–β-catenin antibody, and quantitative PCR analyses were performed with primer against promoter of *CD274*. *, P < 0.01, on the basis of Student's *t* test. **(F)** U87/EGFRvIII cells with stable expression of the β-catenin shRNA and with reconstituted expression of WT rβ-catenin or rβ-catenin S552A mutant were transfected with a luciferase reporter vector containing WT LEF/TCF sequence of *CD274* promoter. These cells were stimulated with or without Wnt3A (20 ng/ml) or EGF (100 ng/ml) for 12 h. Luciferase activity was measured. *, P < 0.01, on the basis of Student's *t* test. **(G)** U87/EGFRvIII cells with stable expression of the β-catenin shRNA were reconstituted with WT rβ-catenin or rβ-catenin S552A mutant expression. The cells were stimulated with or without Wnt3A (20 ng/ml) or EGF (100 ng/ml) for 12 h. ChIP assays with an anti-IgG or anti-Flag antibody and quantitative PCR analyses with primers against promoter of *CD274* were performed. *, P < 0.01, on the basis of Student's *t* test. IP, immunoprecipitation; Mut, mutation.

(-665)-CTTTGAGG-(-658) is a consensus sequence recognized by TCF/LEF (Cadigan and Waterman, 2012; Fig. 3 A). We constructed a luciferase reporter driven by the *CD274* promoter that contains either the WT or a mutated potential TCF/LEF–binding sequence. As shown in Fig. 3 B, treatment of U87/EGFR cells with Wnt3A, EGF, or expression of CA β-catenin significantly increased the activity of the WT but not the mutated promoter. As expected, treatment with Wnt3A or EGF increased the binding of β-catenin to LEF-1 (Fig. S3 A), and depletion of LEF-1 (Fig. S3 B) reduced Wnt3A- or EGF-induced luciferase activity (Fig. S3 C). A chromatin immunoprecipitation (ChIP) assay with an anti–β-catenin or an anti–LEF-1 antibody showed that treatment of U87/EGFR cells with Wnt3A, EGF, or expression of CA β-catenin increased the binding of β-catenin and LEF-1 to the promoter region of *CD274* (Fig. 3 C). MK2206 treatment reduced Wnt3A-, EGF-, or EGFRvIII-induced luciferase activity driven by the *CD274* promoter (Fig. 3 D and Fig. S3 D) and also reduced the binding of β-catenin to the promoter region of *CD274* in U87/EGFR (Fig. 3 E) and U87/EGFRvIII (Fig. S3 E) cells. A similar inhibitory effect was also observed via overexpression of PTEN in EGF-treated U251 and U87 cells (Fig. S3, F and G). In addition, restored expression of the β-catenin S552A mutant reduced Wnt3A- and EGF-induced and *CD274* promoter-mediated luciferase activity and the binding of β-catenin to this promoter region in U87/EGFR cells (Fig. 3, F and G). These results indicate that the β-catenin/TCF/LEF complex binds to the *CD274* promoter region in response to EGFR activation–, PTEN loss–, and Wnt3A-induced AKT activation and enhances *CD274* transcription.

β-Catenin activation promotes immune evasion of tumor cells and brain tumor growth

To determine the effect of β-catenin–regulated PD-L1 expression in tumor cells on T cell activation, we co-cultured Wnt3A-treated

GL261 cells with PMA- and ionomycin-activated mouse primary CD8⁺ T cells and showed that GL261 cell co-culture inhibited *IL-2* (Fig. 4 A) and *IFNγ* (Fig. S4 A) mRNA expression levels in mouse primary CD8⁺ T cells. This inhibition was significantly further enhanced by the expression of PTEN shRNA or CA β-catenin expression in GL261 cells (Fig. 4 A and Fig. S4 A). Similarly, Wnt3A-treated U251 cell co-culture inhibited *IL-2* mRNA expression in PMA- and ionomycin-activated Jurkat T cells (Fig. S4 B), and this inhibition was alleviated by the expression of PTEN or β-catenin shRNA in U251 cells (Fig. S4 B).

GL261 cells predominantly express MHC class I (MHC-I) molecules (Garg et al., 2016). We co-cultured MHC-I–depleted GL261 cells with activated CD4⁺ or CD8⁺ T cells. ELISpot analyses showed that depletion of MHC-I by expressing an shRNA of *H2-K^D*, a gene encoding a subunit of the MHC-I complex, in GL261 cells reduced IL-2 and IFNγ production by CD8⁺ T cells but not CD4⁺ T cells (Fig. S4, C and D). Notably, this reduction was exacerbated by PTEN depletion. These results suggest that CD8⁺ T cell activation can be regulated by both PD-L1 and MHC-I protein expression in tumor cells.

We next examined the role of β-catenin–regulated PD-L1 expression in tumorigenesis and tumor immune evasion in mice. We intracranially injected luciferase-expressing GL261 mouse glioma cells with or without PTEN depletion, CA β-catenin expression, or β-catenin depletion into syngeneic C57BL/6 mice. β-Catenin depletion greatly reduced brain tumor growth (Fig. 4, B and C; and Fig. S4 E) and prolonged mouse survival (Fig. 4 D), whereas PTEN depletion and CA β-catenin expression promoted tumor growth (Fig. 4, B and C; and Fig. S4 E) and shortened mouse survival (Fig. 4 D). IHC staining of tumor tissue showed that PTEN depletion enhanced AKT S473 phosphorylation and β-catenin S552 phosphorylation (Fig. S4 F). In addition, PTEN depletion or CA β-catenin expression increased PD-L1 expression, reduced CD8⁺ T cell infiltration into the tumor tissue (Fig. 4 E), and decreased granzyme B expression, indicating reduced cytotoxic T cell activity (Fig. S4 F). In contrast, β-catenin depletion decreased PD-L1 expression, accompanied by increased CD8⁺ T cell accumulation in the tumor tissue (Fig. 4 E) and increased granzyme B expression (Fig. S4 F). Notably, overexpression of Flag-tagged PD-L1 in β-catenin–depleted GL261 cells largely restored tumor growth and decreased CD8⁺ T cell infiltration (Fig. S4 G). Similar to the effect on tumor growth derived from GL261 cells, β-catenin depletion in CT-2A mouse glioma cells also greatly reduced brain tumor growth (Fig. S4 H, top panel of the mouse images and left panel of the graph) with decreased PD-L1 expression and increased CD8⁺ T cell infiltration (Fig. S4 I).

AKT activation is instrumental for β-catenin–regulated PD-L1 expression, suggesting that AKT inhibition can overcome immune evasion by tumor cells. Intraperitoneal injection of MK2206 or intracranial and intratumoral injection of an anti–PD-1 antibody inhibited GL261 cell–derived tumor growth (Fig. 4, F and G; and Fig. S4 J) and prolonged mouse survival (Fig. 4 H). Similar results were also obtained for CT-2A cell–derived tumor growth (Fig. S4 H, top panel of the mouse images and left panel of the graph) and mouse survival (Fig. S4 K). In addition, an additive effect on tumor growth inhibition and improved mouse survival was observed by combined treatment with MK2206 and the anti–PD-1 antibody (Fig. 4, F–H). Notably, systemic depletion of CD8⁺ T cells using an anti-CD8 antibody treatment (Fig. S4 L) resulted in a reduction in the inhibitory effect of MK2206, anti–PD-1 antibody treatment, and β-catenin depletion on tumor growth (Fig. S4 H, bottom panel of the mouse images and right panel of the graph). Intriguingly, MK2206 treatment-induced inhibition of tumor growth, PD-L1 expression, and CD8⁺ T cell infiltration was abrogated by the expression of active β-catenin in CT-2A cells (Fig. S4 M).

IHC staining of tumor tissue showed that MK2206 treatment inhibited AKT S473 phosphorylation and β-catenin S552 phosphorylation (Fig. S4 N). In addition, MK2206 or an anti–PD-1 antibody treatment reduced PD-L1 expression accompanied by more CD8⁺ T cell infiltration into the tumor tissue (Fig. 4 I) with increased granzyme B expression (Fig. S4 N). These effects were further enhanced by combined treatment with MK2206 and the anti–PD-1 antibody. Together, these results suggest that AKT activates β-catenin, resulting in up-regulated PD-L1 expression and subsequent promotion of tumor cell immune evasion and brain tumor growth.

PD-L1 expression is positively correlated with the levels of β-catenin S552 phosphorylation in human GBM

To determine the clinical relevance of β-catenin–regulated PD-L1 expression, we analyzed The Cancer Genome Atlas (TCGA) data and revealed that GBMs with *PTEN* mutations, which account for ∼30% of GBMs (Cancer Genome Atlas Research Network, 2008; Riddick and Fine, 2011), had higher levels of *CD274* mRNA expression than those with WT PTEN (Fig. 5 A). In addition, the expression levels of the β-catenin downstream genes *LEF-1* and *PPARδ* (Hupe et al., 2017) were positively correlated with *CD274* mRNA expression levels (Fig. S5 A). Consistent with these results, immunoblotting analyses of 10 human GBM specimens showed that AKT S473 phosphorylation, β-catenin S552 phosphorylation, and PD-L1 expression levels were inversely correlated with PTEN expression levels (Fig. 5 B). We also analyzed an additional 39 human GBM specimens with WT PTEN expression with immunoblotting assays and revealed that the levels of EGFR Y1068 phosphorylation, AKT S473 phosphorylation, β-catenin S552 phosphorylation, and PD-L1 expression were positively correlated with each other (Fig. S5 B). These results suggest that AKT activation resulting from mutation of *PTEN* or EGFR activation correlates with the levels of AKT-mediated β-catenin S552 phosphorylation and PD-L1 expression in human GBM.

We next performed IHC analyses of 50 human GBM tissues; the levels of β-catenin S552 phosphorylation were positively correlated with PD-L1 expression and inversely correlated with CD8⁺ T cell infiltration (Fig. 5, C and D). In addition, immunofluorescent analyses showed that active β-catenin and high PD-L1 expression occurred in the same cells of GBM specimens (Fig. S5 C). These results support a role of β-catenin–regulated PD-L1 expression in tumor cell immune evasion in human GBM.

Discussion

Treatments that target immune checkpoints mediated by PD-1 and PD-L1 have been approved for human cancer, with durable clinical benefits (Cabodevilla et al., 2013; Sharma and Allison, 2015).

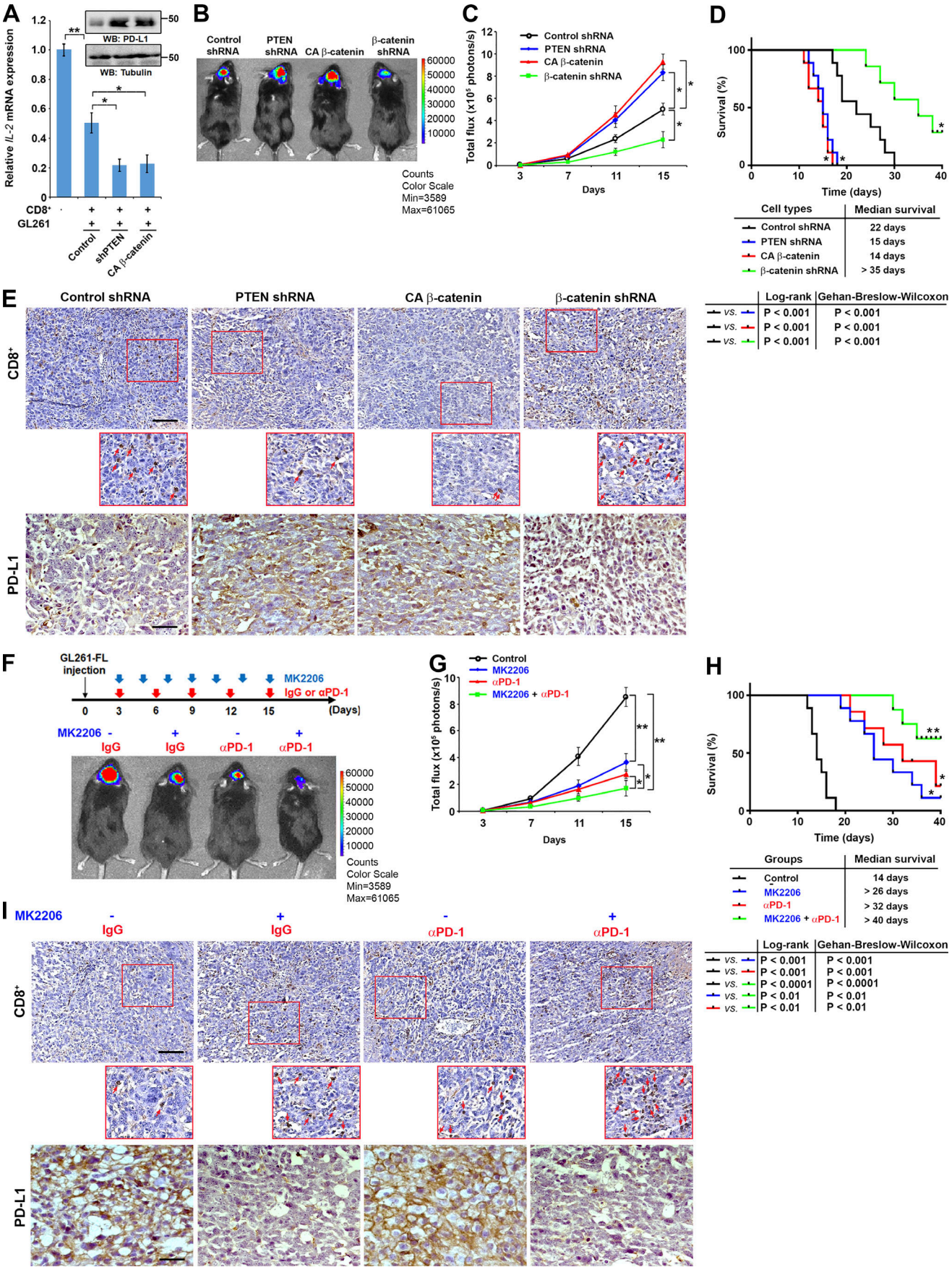
A
Relative IL-2 mRNA expression
WB: PD-L1
WB: Tubulin
CD8+
GL261
Control
shPTEN
CA β-catenin
B
Control shRNA
PTEN shRNA
CA β-catenin
β-catenin shRNA
Counts
Color Scale
Min=3589
Max=61065
C
Control shRNA
PTEN shRNA
CA β-catenin
β-catenin shRNA
Total flux (x10⁵ photons/s)
Days
D
Survival (%)
Time (days)
Cell types | Median survival
Control shRNA | 22 days
PTEN shRNA | 15 days
CA β-catenin | 14 days
β-catenin shRNA | > 35 days
Log-rank | Gehan-Breslow-Wilcoxon
vs. | P < 0.001 | P < 0.001
vs. | P < 0.001 | P < 0.001
vs. | P < 0.001 | P < 0.001
E
Control shRNA
PTEN shRNA
CA β-catenin
β-catenin shRNA
CD8+
PD-L1
F
GL261-FL injection
MK2206
IgG or αPD-1
(Days)
MK2206 - + - +
IgG IgG αPD-1 αPD-1
Counts
Color Scale
Min=3589
Max=61065
G
Control
MK2206
αPD-1
MK2206 + αPD-1
Total flux (x10⁵ photons/s)
Days
H
Survival (%)
Time (days)
Groups | Median survival
Control | 14 days
MK2206 | > 26 days
αPD-1 | > 32 days
MK2206 + αPD-1 | > 40 days
Log-rank | Gehan-Breslow-Wilcoxon
vs. | P < 0.001 | P < 0.001
vs. | P < 0.001 | P < 0.001
vs. | P < 0.0001 | P < 0.0001
vs. | P < 0.01 | P < 0.01
vs. | P < 0.01 | P < 0.01
I
MK2206 - + - +
IgG IgG αPD-1 αPD-1
CD8+
PD-L1

Figure 4. **β-Catenin activation promotes immune evasion of tumor cells and brain tumor growth. (A)** Mouse primary CD8⁺ T cells were preactivated for 12 h with PMA (20 ng/ml) and ionomycin (500 ng/ml) and co-cultured with or without PTEN shRNA or CA β-catenin–expressing GL261 cells that had been pretreated with Wnt3A (20 ng/ml) for 12 h to up-regulate PD-L1 expression. *IL-2* mRNA expression levels in the mouse primary CD8⁺ T cells were measured by real-time PCR analysis 24 h after co-culture. Data represent the means ± SD of three independent experiments. **, P < 0.001; *, P < 0.01, on the basis of one-way ANOVA. **(B–D)** A total of 10^5 FL-expressing GL261 (GL261-FL) cells with or without expression of PTEN shRNA, CA β-catenin, or β-catenin shRNA were intracranially injected into syngeneic C57BL/6 mice. Tumor growth was monitored and analyzed beginning on the fourth day after injection. **(B)** Representative tumor growth was shown in vivo by bioluminescence imaging using IVIS 100 on day 15. **(C)** A bioluminescence imaging analysis of tumor burden was performed on the indicated days. Data represent the means ± SD of nine mice. *, P < 0.001, on the basis of Student's *t* test. **(D)** Top: The mouse survival times were recorded and visualized using Kaplan-Meier survival curves. Bottom: Data represent the means ± SD of nine mice. Tables show the median survival of mice and the P values, which were calculated using the log-rank test and Gehan-Breslow-Wilcoxon test, respectively. *, P < 0.001, on the basis of Student's *t* test. **(E)** The IHC staining of the mouse tumor tissues was performed with the indicated antibodies. Representative images are shown. Scale bar, 100 µm (CD8⁺ images); 50 µm (PD-L1 images). High-magnification images correspond to the areas marked by the red box. Red arrows point to CD8⁺ cells. **(F–H)** 10^5 GL261-FL cells with expression of PTEN shRNA were intracranially injected into syngeneic C57BL/6 mice. Tumor growth was monitored and analyzed beginning on the fourth day after injection. **(F)** Top: The treatment protocol is summarized. Bottom: Representative tumor growth is shown in vivo by bioluminescence imaging using IVIS 100 on day 15. **(G)** A bioluminescence imaging analysis of tumor burden was performed on the indicated days. Data represent the means ± SD of nine mice. *, P < 0.001; **, P < 0.0001 on the basis of Student's *t* test. **(H)** Top: Mouse survival time was recorded and visualized using Kaplan-Meier survival curves. Data represent the means ± SD of nine mice. Bottom: Tables show the median survival of mice and the P values, which were calculated using the log-rank test and Gehan-Breslow-Wilcoxon test, respectively. *, P < 0.001; **, P < 0.0001 on the basis of Student's *t* test. **(I)** The IHC staining of mouse tumor tissues was performed with the indicated antibodies. Representative images are shown. Scale bar, 100 µm (CD8⁺ images); 50 µm (PD-L1 images). High-magnification images correspond to the areas marked by the red box. Red arrows point to CD8⁺ cells. Min, minimum; Max, maximum.

However, the majority of cancer patients are resistant to anti–PD-1/PD-L1 treatment, and the underlying mechanisms of this resistance remain unclear. We demonstrated here that EGFR activation and active Wnt signaling, which occur in a large variety of cancers, induce transcriptional up-regulation of PD-L1 that is directly mediated by the β-catenin/TCF/LEF transcriptional complex. Importantly, AKT activation, which occurs in most cancer cells and is regulated by growth factors, including Wnt ligands, PI3K activation, and PTEN loss, promotes β-catenin–dependent PD-L1 expression and tumor immune evasion (Fig. 5 E). Active β-catenin signaling in melanoma cells promotes T cell exclusion through decreased CCL4 production in tumor cells (Spranger et al., 2015). However, the Wnt–β-catenin pathway does not affect *Ccl4* gene expression in GBM cells, suggesting that CCL4 is not involved in β-catenin–promoted T cell exclusion in the GBM microenvironment.

Inhibition of AKT with MK2206, which is currently in clinical trials for the treatment of cancer (Konopleva et al., 2014), or β-catenin depletion reduces PD-L1 expression levels in tumor cells, enhances CD8⁺ T cell infiltration, and inhibits tumor growth. Alleviation of these effects by the systemic depletion of CD8⁺ T cells further supports a critical role of AKT- and β-catenin transactivation–regulated PD-L1 expression in tumor immunogenicity. As expected, MK2206 combined with an anti–PD-1 antibody, which causes more profound abrogation of immune checkpoint blockade, significantly enhanced CD8⁺ T cell infiltration, and blocked tumor growth. Hence, our findings elucidate a novel mechanism underlying PD-L1 up-regulation that is controlled by widely activated Wnt signaling, EGFR, and AKT and by frequently mutated PTEN; our results also provide a molecular basis for improving the clinical response rate and efficacy of targeted therapy and PD-1/PD-L1 blockade therapy in cancer patients.

Materials and methods

Materials

Normal rabbit immunoglobulin (sc-2027), normal mouse immunoglobulin (sc-2025), anti–H2-K^D antibody (sc-53852; 1:200 for immunoblotting), and anti–β-catenin antibody (sc-7963; 1:200 for immunoblotting and 1:100 for immunoprecipitation) were purchased from Santa Cruz Biotechnology. Rabbit polyclonal antibodies that recognize human β-catenin (9566; 1:1,000 for immunoblotting), active β-catenin (8814; 1:800 for IHC analysis), human PD-L1 (E1L3N, 13684; 1:1,000 for immunoblotting), AKT (pT308, 4056; 1:1,000 for immunoblotting), AKT (pS473, 4060; 1:1,000 for immunoblotting), AKT (9272; 1:1,000 for immunoblotting), PTEN (9559; 1:1,000 for immunoblotting), LEF-1 (76010; 1:1,000 for immunoblotting and 1:100 for immunoprecipitation), and mouse CD8α (98941; 1:400 for IHC analysis) were purchased from Cell Signaling Technology. Mouse monoclonal antibodies for FLAG (F3165, clone M2; 1:5,000 for immunoblotting), HA (H6908; 1:5,000 for immunoblotting), tubulin (T6074, clone B-5-1-2; 1:5,000 for immunoblotting), PMA (P8139), ionomycin (I3909), and actinomycin D (A1410) were purchased from Sigma-Aldrich. Monoclonal antibody for human CD8 (144B, ab17147; 1:50 for IHC analysis) and polyclonal antibody for Granzyme B were obtained from Abcam. Rat anti-mouse PD-1 (BE0146) and anti-mouse PD-L1 (BE0101) were obtained from Bio X Cell. PD-L1 PE-conjugated antibody (MIH1, 12–5983-42; 1:20 for flow cytometry analysis) was purchased from Thermo Fisher Scientific. Human recombinant EGF (01–407) was obtained from EMD Millipore. Puromycin (540222) and G418 (345810) were purchased from EMD Biosciences. Wnt3A (5036-WN-010) was purchased from R&D Systems. D-luciferin (14681) was obtained from Cayman. HyFect transfection reagents (E2650) were obtained from Denville Scientific. LY294002 (L-7988) was purchased from LC Laboratories. MK-2206 (S1078) was purchased from Selleck Chemicals.

Cell culture and transfection

DU145, PC14, and GBM cells, including U251, U87, LN18, EGFR-overexpressing U87 (U87/EGFR), EGFRvIII-overexpressing U87 (U87/EGFRvIII), CT-2A, GL261, and *firefly luciferase* (*FL*)–expressing

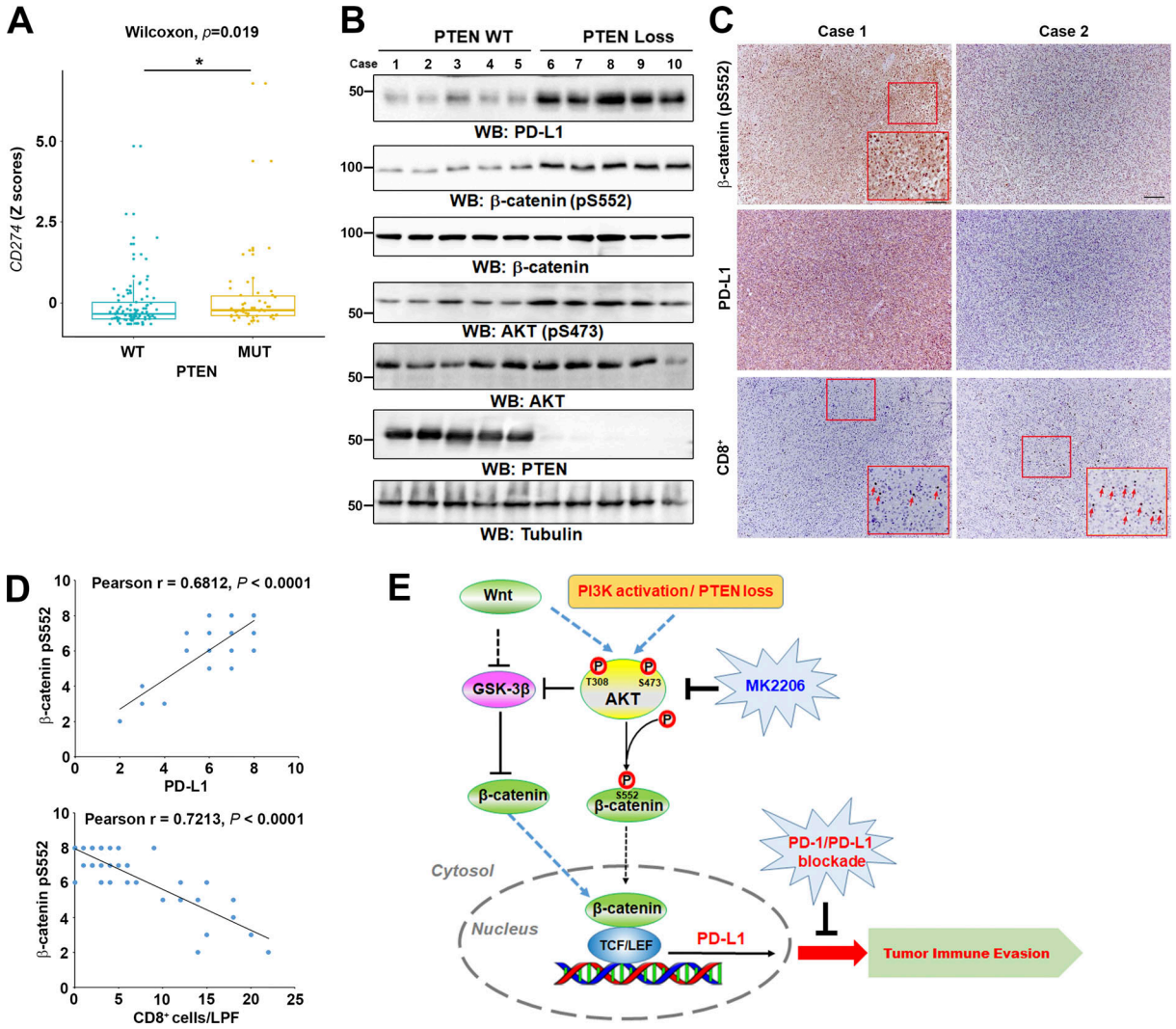

Figure 5. **PD-L1 expression is positively correlated with the levels of β-catenin S552 phosphorylation in human GBM. (A)** TCGA analysis of *CD274* mRNA expression (normalized Z-score) in GBM specimens (n = 145) with (n = 50) or without (n = 95) PTEN mutations was performed. Boxes represent the median and the interquartile range. Error bars are drawn from the 25th to the 75th percentile. The Wilcoxon rank-sum test was used to compare the differences in mRNA expression between two groups (i.e., PTEN mutation vs. WT). *, P < 0.05, on the basis of Student's t test. **(B)** Human GBM specimens were subjected to immunoblotting analysis with the indicated antibodies. **(C)** The IHC staining of 50 human GBM specimens was performed with the indicated antibodies. Scale bar, 100 µm. Red arrows point to $CD8^+$ T cells. **(D)** The IHC staining was scored, and correlation analyses were performed. The Pearson correlation test was used. Note that the scores of some samples overlap. **(E)** A mechanism of tumor immune evasion via transcriptional up-regulation of PD-L1. PD-L1 is transcriptionally enhanced by the β-catenin/TCF/LEF transcriptional complex in response to EGFR-dependent PI3K activation, PTEN loss, and active Wnt singling. Activated AKT activates β-catenin via direct phosphorylation of β-catenin and inhibition of GSK-3β. LPF, low-power field; MUT, mutant; WB, Western blot.

CT-2A and GL261 (CT-2A–FL or GL261-FL) cells were maintained in DMEM or DMEM/F12 supplemented with 10% bovine calf serum (HyClone); these cells are routinely tested for mycoplasma. Human primary GBM cells were maintained in DMEM/F-12 50/50 supplemented with B27, EGF (10 ng/ml), and basic fibroblast growth factor (10 ng/ml). U87 and U251 cells were authenticated using short tandem repeat profiling at The University of Texas MD Anderson Cancer Center Characterized Cell Line Core Facility. Cells were plated at a density of 4×10^5 per 60-mm dish or 10^5 per well of a 6-well plate 18 h before transfection. Transfection was performed using HyFect transfection reagent (Denville Scientific) according to the manufacturer's instructions.

DNA constructs and mutagenesis

PCR-amplified human β-catenin and PD-L1 were cloned into pcDNA3.1/hygro(+)–Flag. The primers for expression plasmid construction were as follows: human PD-L1, 5′-CGGGATCCATGAGGATATTTGCTGTCTT-3′ (forward) and 5′-CCGCTCGAGGCCGTCTCCTCCAAATGTGTAT-3′ (reverse) and human β-catenin, 5′-CGGGATCCATGGCTACTCAAGCTGATTTGATG-3′ (forward) and 5′-CCGCTCGAGGCCAGGTCAGTATCAAACCAGGCCA-3′ (reverse). Human PTEN was cloned by using the following primers: 5′-CGGGATCCATGACAGCCATCATCAAAGAGAT-3′ (forward) and 5′-GACTTTTGTAATTTGTGTATGCTG-3′ (reverse). Then, the PTEN coding sequence was inserted into the PCDH-CMV-MCS-EF1-Puro-SFB vector. pLV/β-catenin

deltaN90 (CA β-catenin) and pECE-Myr-HA-AKT1 (delta4-129) were purchased from Addgene. pcDNA3.1/hygro(+)–Flag β-catenin S552A was created using the QuikChange site-directed mutagenesis kit (Stratagene).

The following pGIPZ shRNAs were used: control shRNA oligonucleotide, 5′-GCTTCTAACACCGGAGGTCTT-3′; mouse PTEN shRNA oligonucleotide, 5′-TATAGGTCAAGTCTAAGTC-3′; human β-catenin shRNA#1 oligonucleotide, 5′-TTACCACTCAGAGAAGGAG-3′, and human β-catenin shRNA#2 oligonucleotide, 5′-TGTGATCCATTCTTGTGCA-3′; human LEF-1 shRNA oligonucleotide, 5′-GCTGGTCTGCAAGAGACAATT-3′; and mouse H2-K^D shRNA oligonucleotide, 5′-AAGAGCGATGAGCAGTGGTTC-3′.

RT and PCR analysis

Total RNA isolation, RT, and real-time PCR were conducted as described previously (Yang et al., 2012b). The following primer pairs were used: human CD274, 5′-CTGCACTTTTAGGAGATTAGATC-3′ (forward) and 5′-CTACACCAAGGCATAATAAGATG-3′ (reverse); human IL-2, 5′-GAATGGAATTAATAATTACAAGAATCCC-3′ (forward) and 5′-TGTTTCAGATCCCTTTAGTTCCAG-3′ (reverse); human Ccl4, 5′-CTCTCAGCACCAATGGGCTC-3′ (forward) and 5′-TCTTTTGGTTTGGAATACCACAG-3′ (reverse); mouse CD274, 5′-GTGAAACCCTGAGTCTTATCC-3′ (forward) and 5′-GACCATTCTGAGACAATTCC-3′ (reverse); mouse Ccl4, 5′-GTTCTCAGCACCAATGGGCTC-3′ (forward) and 5′-TCTTTTGGTCAGGAATACCACAG-3′ (reverse); mouse IL-2, 5′-GCTGTTGATGGACCTACAGGA-3′ (forward) and 5′-ATCCTGGGGAGTTTCAGGTT-3′ (reverse); β-actin, 5′-ATGGATGACGATATCGCTGCGC-3′ (forward) and 5′-GCAGCACAGGGTGCTCCTCA-3′ (reverse); and mouse IFNγ, 5′-GCATCTTGGCTTTGCAGCT-3′ (forward) and 5′-CCTTTTTCGCCTTGCTGTTG-3′ (reverse).

Immunoblot analysis

Extraction of proteins from cultured cells was performed using lysis buffer (50 mM Tris-HCl [pH 7.5], 0.1% SDS, 1% Triton X-100, 150 mM NaCl, 1 mM dithiothreitol, 0.5 mM EDTA, 100 µM PMSF, 100 µM leupeptin, 1 µM aprotinin, 100 µM sodium orthovanadate, 100 µM sodium pyrophosphate, and 1 mM sodium fluoride). Cell extracts were clarified via centrifugation at 13,400 *g*, and the supernatants (2 mg protein/ml) were subjected to immunoblot analysis with the corresponding antibodies. The band intensity was quantified using the Image Lab software program (Bio-Rad). Each experiment was repeated at least three times.

Flow cytometry analysis

Cells were washed in PBS and stained for cell surface PD-L1 on ice for 30 min in FACS blocking buffer (0.5% BSA and 2% FBS in PBS). PD-L1 PE-conjugated antibody was added to the cells on ice for 30 min. After incubation, the cells were washed with FACS buffer (0.5% BSA in PBS) three times and detected by a BD FACSCelesta (BD Biosciences) cytometer. The results were analyzed by FlowJo v10.

Luciferase reporter assay

The human *CD274* promoter was cloned from the genomic DNA of U87 cells. The following primers were used: 5′-CGGGGTACCATGTAGCTCGGGATGGGAAGT-3′ (forward) and 5′-CCGCTCGAGCTCTGCCCAAGGCAGCAAATC-3′ (reverse). The amplified clone corresponding to the human *CD274* promoter (600 bp upstream of the transcription start site) containing the TCF/LEF sequence was inserted into the KpnI/XhoI sites of the pGL3-Basic vector (Promega). Site-directed mutagenesis was performed using 5′-GTCGAGGAACTGGAAGGAAGTCACAG-3′ (forward) and 5′-CTGTGACTTCCTTCCAGTTCCTCGAC-3′ (reverse) primers and verified by sequencing. The tumor cells were cotransfected with 1 µg of pGL3 empty vector, pGL3 WT TCF/LEF, or pGL3 TCF/LEF mutant vectors and 0.5 µg of pRL-TK vector (as an inner control that contains Renilla luciferase sequences; Promega) by Lipofectamine 2000 (Invitrogen) and grown under different experimental conditions. After incubation, firefly and Renilla luciferase activities were measured using the dual-luciferase reporter assay (Promega), and the ratio of firefly/Renilla luciferase was determined.

ChIP assay

A ChIP assay was performed using the SimpleChIP Enzymatic Chromatin IP kit (9003; Cell Signaling Technology). Chromatin prepared from cells (in a 10-cm dish) was used to determine the total DNA input and was incubated overnight with specific antibodies or with normal rabbit or mouse IgG. The immunoprecipitated chromatin was analyzed using a CFX96 real-time PCR detection system (Bio-Rad). The PCR primer sequences for the *CD274* promoter were 5′-ATGTAGCTCGGGATGGGAAGT-3′ (forward) and 5′-TGTGTGTGTGTGTATGGGTGTA-3′ (reverse).

Co-culture experiments

GL261 or U251 cells, with or without expression of PTEN shRNA, S protein tag/Flag tag/Streptavidin binding peptide (SFB)–PTEN, CA β-catenin, or β-catenin shRNA, were treated with Wnt3A (20 ng/ml) for 12 h before being co-cultured with mouse primary $CD8^+$ T cells or Jurkat T cells that had been activated with PMA (20 ng/ml) and ionomycin (500 ng/ml) for 12 h at a ratio of 4:1 (T cells:tumor cells) for 24 h. The T cells were then collected to analyze *IL-2* mRNA expression.

ELISpot assay

The 10^8 GL261 cells were collected and resuspended in DMEM. These cells were then frozen in a −80°C freezer for 1 h and thawed at 37°C for three cycles to lyse the cells. The solution was centrifuged at 300 rpm for 30 min, and the supernatants were collected and stored at 4°C for further use as tumor-specific antigens.

The mice were euthanized, and the spleens were collected. The spleens were disassociated by squeezing, and all released and suspended cells were collected. The suspended cells were treated with red cell lysis buffer (Beyotime), and the splenocytes were centrifuged at 400 *g* for 3 min. The splenocytes were cultured with GL261 cell lysates (1:3 for the cell numbers) for 48 h. The lymphocytes were isolated from cultured splenocytes using gradient centrifugation on histopaque-1077. $CD4^+$ T and $CD8^+$ T cells were isolated from lymphocytes according to the instructions of $CD4^+$ or $CD8^+$ T cell isolation kits (Miltenyi Biotec).

GL261 cells expressing a control shRNA or H2-K^D shRNA (MHC-I subunit) were infected with lentivirus expressing *PTEN* shRNA. $CD4^+$ or $CD8^+$ T cells were co-cultured with GL261 cells at a ratio of 3:1 for 24 h, and $CD4^+$ or $CD8^+$ T cells were then collected and subjected to ELISpot analysis with an ELISpot kit (R&D Systems) containing plates coated with an anti–IFNγ or an anti–IL-2 antibody.

Animal experiments

We intracranially injected 10^5 GL261-FL cells (in 5 µl of DMEM/F12 per mouse), with or without expression of PTEN shRNA, CA β-catenin, or β-catenin shRNA, into 4-wk-old male C57BL/6 mice. We divided the mice into two groups. One group consisted of seven mice in each subgroup and was used to monitor tumor growth and perform IHC analyses. The mice were euthanized 15 d after the GL261-FL cells were injected. The brain of each mouse was harvested, fixed in 4% formaldehyde, and embedded in paraffin. Tumor formation and phenotype were determined by bioluminescence imaging and histological analysis of hematoxylin and eosin–stained sections.

The other groups, which consisted of nine mice in each subgroup, were monitored for survival. The results were analyzed using STATISTICA software and presented in Kaplan-Meier plots. Humane endpoints included weight loss of 20–25%, weakness that prevented them from obtaining food or water, loss of appetite (anorexia for 24 h), a moribund state, and an inability to participate in normal activities because of tumor growth. All mice were euthanized under anesthesia after two or more of these humane endpoints had been observed.

For treatment with MK2206 and antibody, 100 mg of anti–PD-1 antibody (RMP1-14; Bio X Cell) or rat IgG (Bio X Cell) as a control was injected intratumorally on days 3, 7, 11, and 15 after GL261-FL cell inoculation, and MK2206 (120 mg/kg) was injected intraperitoneally on days 3, 5, 7, 9, 11, 13, and 15.

All of the mice were housed in the MD Anderson Cancer Center animal facility (Houston, TX); all experiments were performed in accordance with relevant institutional and national guidelines and regulations and were approved by the Institutional Animal Care and Use Committee at the MD Anderson Cancer Center.

In vivo depletion of $CD8^+$ T cells

C57BL/6 male mice were intraperitoneally injected with 200 mg anti-CD8 antibody (Clone 2.43) or rat IgG isotype. To determine the efficiency of depletion, spleens were collected from the mice at day 3 after injection, and then the lymphocytes were isolated from the spleen cells by using gradient centrifugation on histopaque-1077 (Sigma-Aldrich). The lymphocytes were incubated with anti-CD3e antibody (145-C11; Thermo Fisher Scientific), anti-CD4 antibody (GK1.5; Thermo Fisher Scientific), and anti-CD8 antibody (53–6.7; Thermo Fisher Scientific), and then the amounts of subpopulation were quantified by flow cytometry.

Bioluminescence imaging and analysis

C57BL/6 mice were intraperitoneally injected with 150 mg/kg D-luciferin in PBS 10 min before bioluminescence imaging. Imaging was conducted using a charge-coupled device camera (IVIS 100, Xenogen; exposure time of 1 min, binning of 8, field of view of 15 cm, f/stop of 1, and no filter). Mice were anesthetized with isoflurane (2% vaporized in O_2) and shaved to minimize attenuation of the signal by pigmented black hair. For analysis, total photon flux (photons per second) was measured from a fixed region of interest using Living Image software (Xenogen). Bioluminescent signals within the fixed region of interest were normalized to the background luminescence and were obtained over the same region of interest from animals that had not been injected with D-luciferin.

IHC analysis and scoring

IHC staining was performed using the VECTASTAIN ABC kit (Vector Laboratories) according to the manufacturer's instructions. Sections of paraffin-embedded xenograft tumors were stained with antibodies against PD-L1 (mouse), AKT (pS473), β-catenin (pS552), CD8α (mouse), Granzyme B, and nonspecific IgG as a negative control. The paraffin-embedded human GBM tumor sections were stained with antibodies against β-catenin (pS552), human PD-L1, active β-catenin, and CD8 (human) with nonspecific IgG as a negative control. We quantitatively scored the tissue sections according to the percentage of positive cells and staining intensity. We assigned the following proportion scores: 0 if 0% of the tumor cells showed positive staining, 0.1–1.0 if 0.1–1% of cells showed positive staining, 1.1–2.0 if 1.1–10% showed positive staining, 2.1–3.0 if 11–30% showed positive staining, 3.1–4.0 if 31–70% showed positive staining, and 4.1–5.0 if 71–100% showed positive staining. We rated the intensity of staining on a scale of 0 to 3: 0, negative; 1, weak; 2, moderate; and 3, strong. We then combined the proportion and intensity scores to obtain a total score (range, 0–8). The total number of intratumoral $CD8^+$ T cells was counted in six low-power fields and presented as an average number of $CD8^+$ T cells per low-power field. All GBM patients from whom the tumor samples were obtained had undergone standard radiotherapy after surgery followed by treatment with an alkylating agent (temozolomide in most cases). Consent for collection of patient specimens, the use of human brain tumor specimens, and the database was approved by the MD Anderson Institutional Review Board.

TCGA analyses

The mRNA expression of *CD274*, *LEF-1*, and *PPARδ* and somatic mutations in *PTEN* in GBM specimens were downloaded from cBioPortal (https://www.cbioportal.org/; Cerami et al., 2012). The mRNA expression of *CD274*, *LEF-1*, and *PPARδ* was normalized to the Z-score, and the correlative expression of these genes was analyzed.

According to somatic mutations in PTEN, GBM samples were classified into two groups: samples with and without nonsynonymous mutations in PTEN. Nonsynonymous mutations include missense mutations, nonsense mutations, splicing mutations, in-frame insertions and deletions, and frameshift insertions and deletions. The Wilcoxon rank-sum test was used to compare the differences in *CD274* mRNA expression between the two groups.

Statistical analysis

All quantitative data are presented as the mean ± SD of at least three independent experiments. A two-group comparison was conducted using a two-sided, two-sample Student's *t* test. A simultaneous comparison of more than two groups was conducted using one-way ANOVA (SPSS statistical package, version 12; SPSS Inc.). Values of $P < 0.05$ were considered statistically significant.

Online supplemental material

Fig. S1 shows that Wnt-induced β-catenin activation results in PD-L1 up-regulation in tumor cells. Fig. S2 shows that AKT activation induced by EGFR-dependent PI3K activation, PTEN loss, and Wnt3A enhances PD-L1 expression in a β-catenin–dependent manner. Fig. S3 shows that the β-catenin/TCF/LEF complex binds to the *CD274* promoter region in response to AKT activation and enhances *CD274* transcription. Fig. S4 shows that β-catenin activation promotes immune evasion of tumor cells and brain tumor growth. Fig. S5 shows that PD-L1 expression is positively correlated with the levels of β-catenin S552 phosphorylation in human GBM.

Acknowledgments

This work was supported by the Zhejiang University Research Fund (188020*194221901/029; to Z. Lu); the Leading Innovative and Entrepreneur Team Introduction Program of Zhejiang (2019R01001; to Z. Lu); the National Research Foundation of Korea grant funded by the Korean government (MIST; 2020R1C1C1011350); the Bio&Medical Technology Development Program funded by the Ministry of Science, ICT and Future Planning, Republic of Korea (NRF-2017M3A9E4047243); National Natural Science Foundation of China (81902151; to L. Du); and Zhejiang Natural Science Foundation grant LQ19H160010 (to L. Du). Z. Lu is a Kuancheng Wang Distinguished Chair.

Author contributions: Z. Lu, J. Lyu, L. Du, and J.-H. Lee conceived and designed the study. L. Du, J.-H. Lee, H. Jiang, C. Wang, S. Wang, D. Xu, J. Li, X. Qian, and X. Li performed experiments. Z. Zheng and F. Shao performed TCGA database analysis. Y. Xia, Y. Zheng, H.-R. Kim, D. Xing, and P. Liu provided reagents and technical assistance. L. Du, J.-H. Lee, J. Lyu, and Z. Lu wrote the paper with comments from all authors. Z. Lu and J. Lyu supervised the entire project.

Disclosures: The authors declare no competing interests exist.

Submitted: 18 June 2019
Revised: 13 March 2020
Accepted: 22 April 2020

References

Anastas, J.N., and R.T. Moon. 2013. WNT signalling pathways as therapeutic targets in cancer. *Nat. Rev. Cancer*. 13:11–26. https://doi.org/10.1038/nrc3419

Boussiotis, V.A.. 2016. Molecular and Biochemical Aspects of the PD-1 Checkpoint Pathway. *N. Engl. J. Med*. 375:1767–1778. https://doi.org/10.1056/NEJMra1514296

Cabodevilla, A.G., L. Sánchez-Caballero, E. Nintou, V.G. Boiadjieva, F. Picatoste, A. Gubern, and E. Claro. 2013. Cell survival during complete nutrient deprivation depends on lipid droplet-fueled β-oxidation of fatty acids. *J. Biol. Chem*. 288:27777–27788. https://doi.org/10.1074/jbc.M113.466656

Cadigan, K.M., and M.L. Waterman. 2012. TCF/LEFs and Wnt signaling in the nucleus. *Cold Spring Harb. Perspect. Biol*. 4. a007906. https://doi.org/10.1101/cshperspect.a007906

Cancer Genome Atlas Research Network. 2008. Comprehensive genomic characterization defines human glioblastoma genes and core pathways. *Nature*. 455:1061–1068. https://doi.org/10.1038/nature07385

Casey, S.C., L. Tong, Y. Li, R. Do, S. Walz, K.N. Fitzgerald, A.M. Gouw, V. Baylot, I. Gütgemann, M. Eilers, et al. 2016. MYC regulates the antitumor immune response through CD47 and PD-L1. *Science*. 352:227–231. https://doi.org/10.1126/science.aac9935

Cerami, E., J. Gao, U. Dogrusoz, B.E. Gross, S.O. Sumer, B.A. Aksoy, A. Jacobsen, C.J. Byrne, M.L. Heuer, E. Larsson, et al. 2012. The cBio cancer genomics portal: an open platform for exploring multidimensional cancer genomics data. *Cancer Discov*. 2:401–404. https://doi.org/10.1158/2159-8290.CD-12-0095

Coelho, M.A., S. de Carné Trécesson, S. Rana, D. Zecchin, C. Moore, M. Molina-Arcas, P. East, B. Spencer-Dene, E. Nye, K. Barnouin, et al. 2017. Oncogenic RAS Signaling Promotes Tumor Immunoresistance by Stabilizing PD-L1 mRNA. *Immunity*. 47:1083–1099.e6. https://doi.org/10.1016/j.immuni.2017.11.016

Dorand, R.D., J. Nthale, J.T. Myers, D.S. Barkauskas, S. Avril, S.M. Chirieleison, T.K. Pareek, D.W. Abbott, D.S. Stearns, J.J. Letterio, et al. 2016. Cdk5 disruption attenuates tumor PD-L1 expression and promotes antitumor immunity. *Science*. 353:399–403. https://doi.org/10.1126/science.aae0477

Esen, E., J. Chen, C.M. Karner, A.L. Okunade, B.W. Patterson, and F. Long. 2013. WNT-LRP5 signaling induces Warburg effect through mTORC2 activation during osteoblast differentiation. *Cell Metab*. 17:745–755. https://doi.org/10.1016/j.cmet.2013.03.017

Fang, D., D. Hawke, Y. Zheng, Y. Xia, J. Meisenhelder, H. Nika, G.B. Mills, R. Kobayashi, T. Hunter, and Z. Lu. 2007. Phosphorylation of beta-catenin by AKT promotes beta-catenin transcriptional activity. *J. Biol. Chem*. 282:11221–11229. https://doi.org/10.1074/jbc.M611871200

Garg, A.D., L. Vandenberk, C. Koks, T. Verschuere, L. Boon, S.W. Van Gool, and P. Agostinis. 2016. Dendritic cell vaccines based on immunogenic cell death elicit danger signals and T cell-driven rejection of high-grade glioma. *Sci. Transl. Med*. 8:328ra27. https://doi.org/10.1126/scitranslmed.aae0105

Guo, W., Z. Keckesova, J.L. Donaher, T. Shibue, V. Tischler, F. Reinhardt, S. Itzkovitz, A. Noske, U. Zürrer-Härdi, G. Bell, et al. 2012. Slug and Sox9 cooperatively determine the mammary stem cell state. *Cell*. 148:1015–1028. https://doi.org/10.1016/j.cell.2012.02.008

Herbst, R.S., J.C. Soria, M. Kowanetz, G.D. Fine, O. Hamid, M.S. Gordon, J.A. Sosman, D.F. McDermott, J.D. Powderly, S.N. Gettinger, et al. 2014. Predictive correlates of response to the anti-PD-L1 antibody MPDL3280A in cancer patients. *Nature*. 515:563–567. https://doi.org/10.1038/nature14011

Hupe, M., M.X. Li, S. Kneitz, D. Davydova, C. Yokota, J. Kele, B.. Hot, J.M. Stenman, and M. Gessler. 2017. Gene expression profiles of brain endothelial cells during embryonic development at bulk and single-cell levels. *Sci. Signal*. 10. https://doi.org/10.1126/scisignal.aag2476

Iwai, Y., M. Ishida, Y. Tanaka, T. Okazaki, T. Honjo, and N. Minato. 2002. Involvement of PD-L1 on tumor cells in the escape from host immune system and tumor immunotherapy by PD-L1 blockade. *Proc. Natl. Acad. Sci. USA*. 99:12293–12297. https://doi.org/10.1073/pnas.192461099

Ji, H., J. Wang, H. Nika, D. Hawke, S. Keezer, Q. Ge, B. Fang, X. Fang, D. Fang, D.W. Litchfield, et al. 2009. EGF-induced ERK activation promotes CK2-mediated disassociation of alpha-Catenin from beta-Catenin and transactivation of beta-Catenin. *Mol. Cell*. 36:547–559. https://doi.org/10.1016/j.molcel.2009.09.034

Kim, J.H., S.Y. Park, Y. Jun, J.Y. Kim, and J.S. Nam. 2017. Roles of Wnt Target Genes in the Journey of Cancer Stem Cells. *Int. J. Mol. Sci*. 18:1604. https://doi.org/10.3390/ijms18081604

Konopleva, M.Y., R.B. Walter, S.H. Faderl, E.J. Jabbour, Z. Zeng, G. Borthakur, X. Huang, T.M. Kadia, P.P. Ruvolo, J.B. Feliu, et al. 2014. Preclinical and early clinical evaluation of the oral AKT inhibitor, MK-2206, for the treatment of acute myelogenous leukemia. *Clin. Cancer Res*. 20:2226–2235. https://doi.org/10.1158/1078-0432.CCR-13-1978

Kuan, C.T., C.J. Wikstrand, and D.D. Bigner. 2001. EGF mutant receptor vIII as a molecular target in cancer therapy. *Endocr. Relat. Cancer*. 8:83–96. https://doi.org/10.1677/erc.0.0080083

Lee, J.H., R. Liu, J. Li, C. Zhang, Y. Wang, Q. Cai, X. Qian, Y. Xia, Y. Zheng, Y. Piao, et al. 2017. Stabilization of phosphofructokinase 1 platelet isoform by AKT promotes tumorigenesis. *Nat. Commun.* 8:949. https://doi.org/10.1038/s41467-017-00906-9

Li, C.W., S.O. Lim, W. Xia, H.H. Lee, L.C. Chan, C.W. Kuo, K.H. Khoo, S.S. Chang, J.H. Cha, T. Kim, et al. 2016. Glycosylation and stabilization of programmed death ligand-1 suppresses T-cell activity. *Nat. Commun.* 7: 12632. https://doi.org/10.1038/ncomms12632

Lim, S.O., C.W. Li, W. Xia, J.H. Cha, L.C. Chan, Y. Wu, S.S. Chang, W.C. Lin, J.M. Hsu, Y.H. Hsu, et al. 2016. Deubiquitination and Stabilization of PD-L1 by CSN5. *Cancer Cell.* 30:925–939. https://doi.org/10.1016/j.ccell.2016.10.010

Lu, Z., and T. Hunter. 2004. Wnt-independent beta-catenin transactivation in tumor development. *Cell Cycle.* 3:571–573. https://doi.org/10.4161/cc.3.5.885

Lu, Z., S. Ghosh, Z. Wang, and T. Hunter. 2003. Downregulation of caveolin-1 function by EGF leads to the loss of E-cadherin, increased transcriptional activity of beta-catenin, and enhanced tumor cell invasion. *Cancer Cell.* 4:499–515. https://doi.org/10.1016/S1535-6108(03)00304-0

MacDonald, B.T., K. Tamai, and X. He. 2009. Wnt/beta-catenin signaling: components, mechanisms, and diseases. *Dev. Cell.* 17:9–26. https://doi.org/10.1016/j.devcel.2009.06.016

Nusse, R., and H. Clevers. 2017. Wnt/β-Catenin Signaling, Disease, and Emerging Therapeutic Modalities. *Cell.* 169:985–999. https://doi.org/10.1016/j.cell.2017.05.016

Parsa, A.T., J.S. Waldron, A. Panner, C.A. Crane, I.F. Parney, J.J. Barry, K.E. Cachola, J.C. Murray, T. Tihan, M.C. Jensen, et al. 2007. Loss of tumor suppressor PTEN function increases B7-H1 expression and immunoresistance in glioma. *Nat. Med.* 13:84–88. https://doi.org/10.1038/nm1517

Riddick, G., and H.A. Fine. 2011. Integration and analysis of genome-scale data from gliomas. *Nat. Rev. Neurol.* 7:439–450. https://doi.org/10.1038/nrneurol.2011.100

Sharma, P., and J.P. Allison. 2015. The future of immune checkpoint therapy. *Science.* 348:56–61. https://doi.org/10.1126/science.aaa8172

Sharma, P., S. Hu-Lieskovan, J.A. Wargo, and A. Ribas. 2017. Primary, Adaptive, and Acquired Resistance to Cancer Immunotherapy. *Cell.* 168: 707–723. https://doi.org/10.1016/j.cell.2017.01.017

Spranger, S., R. Bao, and T.F. Gajewski. 2015. Melanoma-intrinsic β-catenin signalling prevents anti-tumour immunity. *Nature.* 523:231–235. https://doi.org/10.1038/nature14404

Yang, W., Y. Xia, H. Ji, Y. Zheng, J. Liang, W. Huang, X. Gao, K. Aldape, and Z. Lu. 2011. Nuclear PKM2 regulates β-catenin transactivation upon EGFR activation. *Nature.* 480:118–122. https://doi.org/10.1038/nature10598

Yang, W., Y. Xia, Y. Cao, Y. Zheng, W. Bu, L. Zhang, M.J. You, M.Y. Koh, G. Cote, K. Aldape, et al. 2012a. EGFR-induced and PKCε monoubiquitylation-dependent NF-κB activation upregulates PKM2 expression and promotes tumorigenesis. *Mol. Cell.* 48:771–784. https://doi.org/10.1016/j.molcel.2012.09.028

Yang, W., Y. Xia, D. Hawke, X. Li, J. Liang, D. Xing, K. Aldape, T. Hunter, W.K. Alfred Yung, and Z. Lu. 2012b. PKM2 phosphorylates histone H3 and promotes gene transcription and tumorigenesis. *Cell.* 150:685–696. https://doi.org/10.1016/j.cell.2012.07.018

Zhang, J., X. Bu, H. Wang, Y. Zhu, Y. Geng, N.T. Nihira, Y. Tan, Y. Ci, F. Wu, X. Dai, et al. 2018. Cyclin D-CDK4 kinase destabilizes PD-L1 via cullin 3-SPOP to control cancer immune surveillance. *Nature.* 553:91–95. https://doi.org/10.1038/nature25015

Supplemental material

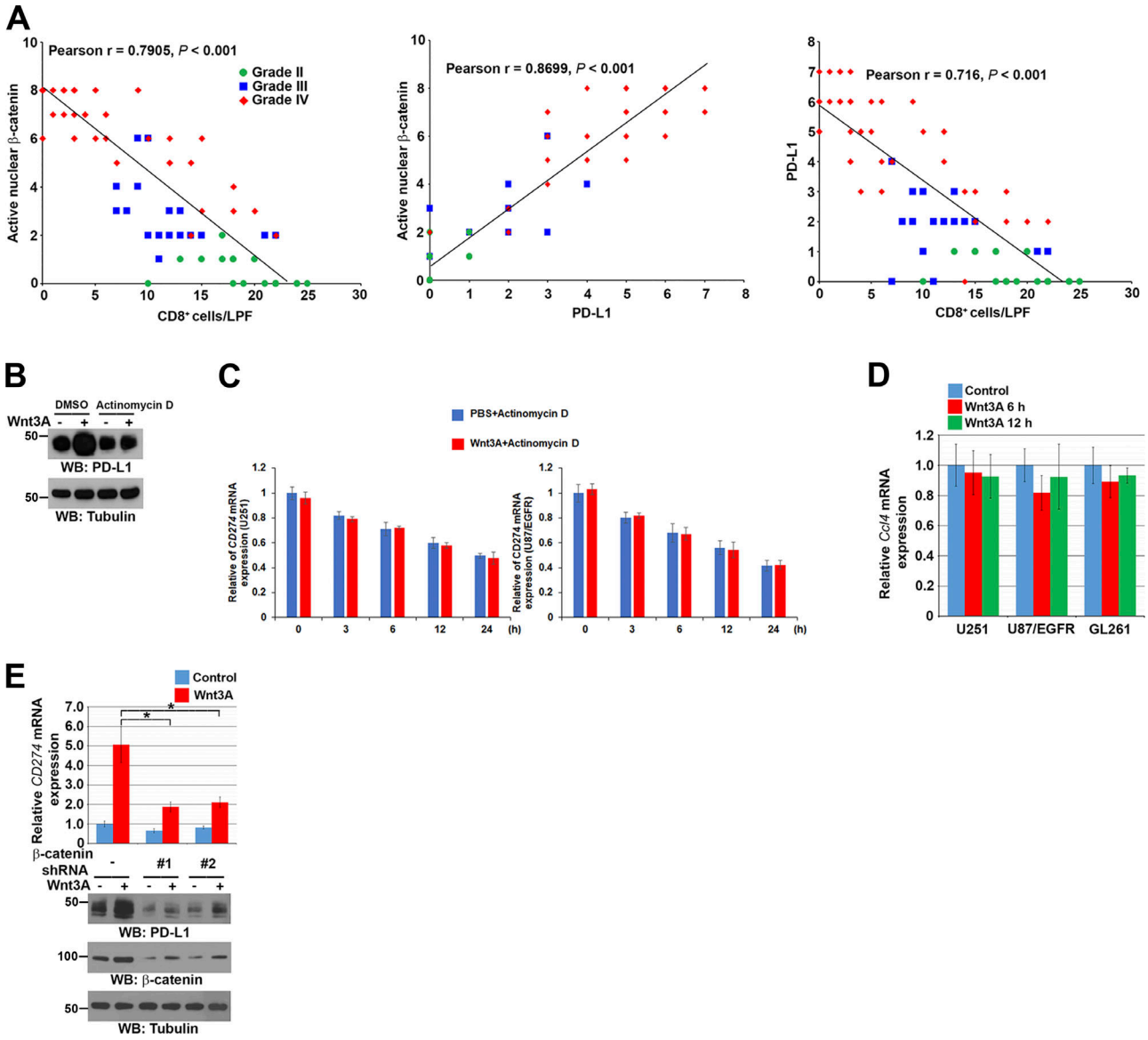

Figure S1. **Wnt-induced β-catenin activation results in PD-L1 up-regulation in tumor cells. (A)** The IHC stains in Fig. 1 A were scored, and correlation analyses were performed. A Pearson correlation test was used. Note that the scores of some samples overlap. **(B)** Serum-starved U251 cells were pretreated with or without actinomycin D (1 µg/ml) for 2 h and then stimulated with or without Wnt3A (20 ng/ml) for 12 h. Immunoblotting analyses were performed with the indicated antibodies. **(C)** U251 and U87/EGFR cells were treated with or without Wnt3A (20 ng/ml) for the indicated periods of time in the presence of actinomycin D (1 µg/ml). Real-time PCR analyses were performed. **(D)** The indicated tumor cells were serum starved for 12 h and then stimulated with or without Wnt3A (20 ng/ml) for the indicated periods of time. Real-time PCR analyses were performed. **(E)** U251 cells with or without stable expression of β-catenin shRNA or a control shRNA were treated with or without Wnt3A (20 µg/ml) for 12 h. A real-time PCR analysis (top) and immunoblotting analyses (bottom) were performed. Data represent the means ± SD of three independent experiments. *, P < 0.0001, on the basis of Student's *t* test. LPF, low-power field; WB, Western blot.

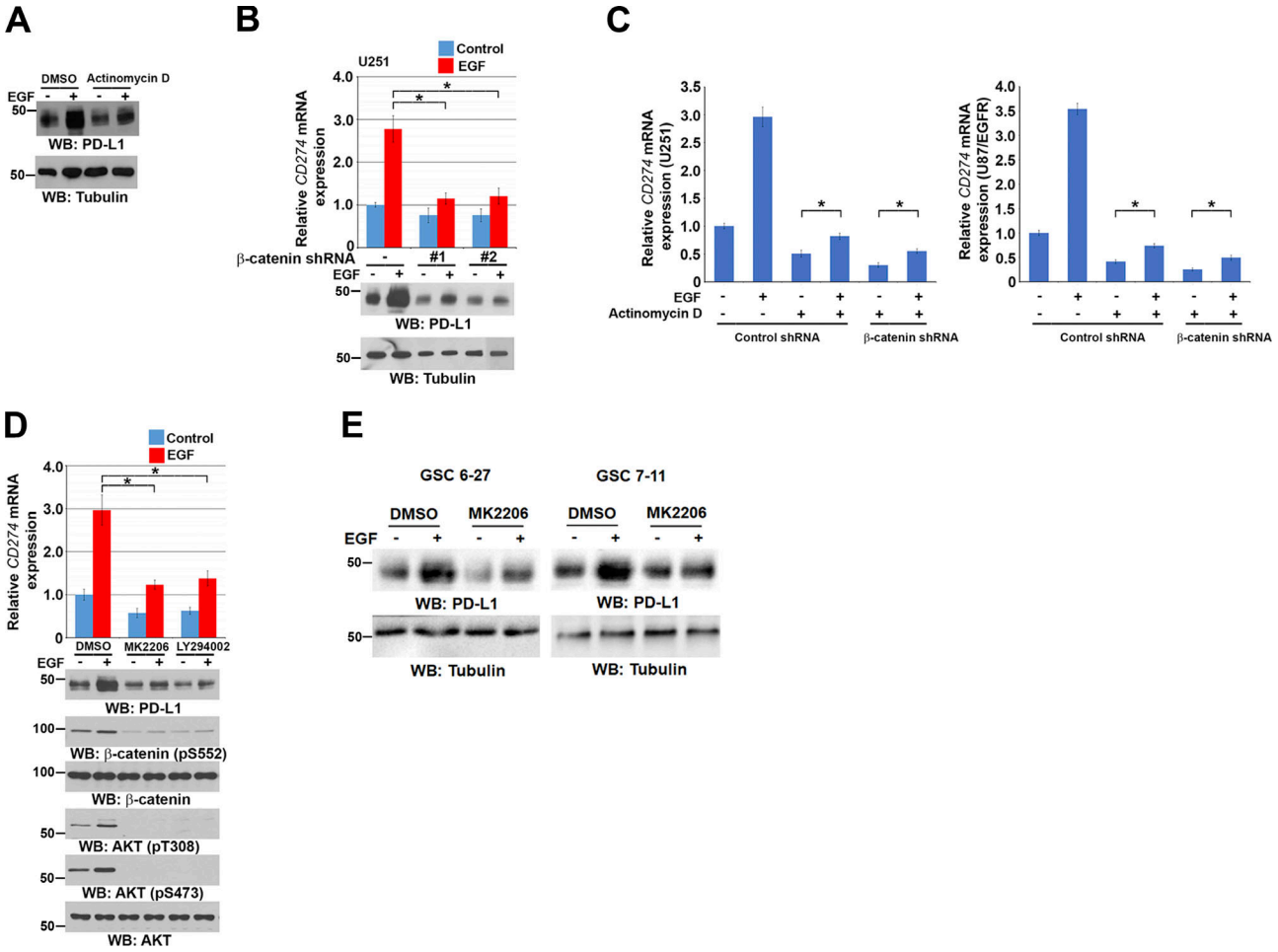

Figure S2. **AKT activation induced by EGFR-dependent PI3K activation, PTEN loss, and Wnt3A enhances PD-L1 expression in a β-catenin–dependent manner. (A)** Serum-starved U251 cells were pretreated with or without actinomycin D (1 µg/ml) for 2 h and then stimulated with or without EGF (100 ng/ml) for 12 h. Immunoblotting analyses were performed with the indicated antibodies. **(B)** U251 cells with stable expression of a β-catenin shRNA or a control shRNA were treated with or without EGF (100 ng/ml) for 12 h. Real-time PCR analyses were performed. Data represent the means ± SD of three independent experiments. *, P < 0.0001, on the basis of Student's *t* test. Immunoblotting analyses were performed with the indicated antibodies. **(C)** U251 and U87/EGFR cells with stable expression of a β-catenin shRNA or a control shRNA were treated with or without EGF (100 ng/ml) for 12 h in the presence or absence of actinomycin D (1 µg/ml). Real-time PCR analyses were performed. Data represent the means ± SD of three independent experiments. *, P < 0.0001, on the basis of Student's *t* test. **(D)** Serum-starved U251 cells were pretreated with DMSO, MK2206 (5 µM), or LY294002 (20 µM) for 2 h and then stimulated with or without EGF (100 ng/ml) for 12 h. Real-time PCR analyses were performed. Data represent the means ± SD of three independent experiments. *, P < 0.0001, on the basis of Student's *t* test. Immunoblotting analyses were performed with the indicated antibodies. **(E)** GSC 6–27 and GSC 7–11 human primary GBM cells were pretreated with DMSO or MK2206 (5 µM) for 2 h and then stimulated with or without EGF (100 ng/ml) for 12 h. Immunoblotting analyses were performed with the indicated antibodies. WB, Western blot.

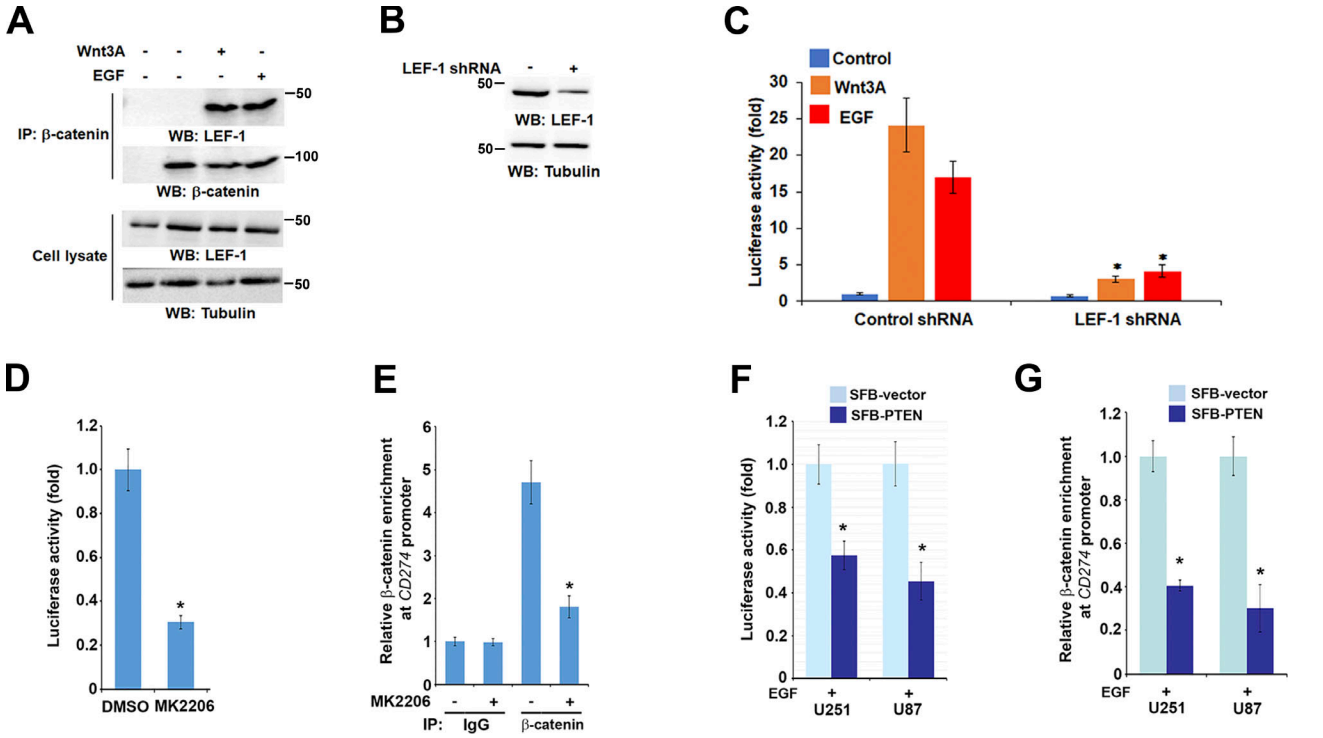

Figure S3. **β-catenin/TCF/LEF complex binds to the *CD274* promoter region in response to AKT activation and enhances *CD274* transcription. (C–G)** Data represent the means ± SD of three independent experiments. **(A)** Serum-starved U251 cells were stimulated with or without Wnt3A (20 ng/ml) or EGF (100 ng/ml) for 6 h. Immunoprecipitation analyses were performed with an anti–β-catenin antibody. Immunoblotting analyses were conducted with the indicated antibodies. **(B)** U251 cells were stably expressed with LEF-1 shRNA or a control shRNA. Immunoblotting analyses were performed with the indicated antibodies. **(C)** U251 cells with stable expression of the LEF-1 shRNA or a control shRNA were transfected with a luciferase reporter vector containing the WT LEF/TCF sequence of *CD274* promoter. These cells were stimulated with or without Wnt3A (20 ng/ml) or EGF (100 ng/ml) for 12 h. Luciferase activity was measured. *, $P < 0.01$, on the basis of Student's *t* test. **(D)** U87/EGFRvIII cells with expression of a luciferase reporter vector containing WT LEF/TCF sequence of *CD274* promoter were treated with or without MK2206 (5 μM) for 12 h. Luciferase activity was measured. *, $P < 0.001$, on the basis of Student's *t* test. **(E)** U87/EGFRvIII cells were treated with or without MK2206 (5 μM) for 12 h. ChIP assays with an anti-IgG or anti–β-catenin antibody and quantitative PCR analyses with primers against promoter of *CD274* were performed. *, $P < 0.001$, on the basis of Student's *t* test. **(F)** U251 and U87 cells were cotransfected with a luciferase reporter vector containing WT LEF/TCF sequence of *CD274* promoter and an SFB-tagged control vector or a vector expressing SFB-PTEN. These cells were stimulated with EGF (100 ng/ml) for 12 h. Luciferase activity was measured. *, $P < 0.001$, on the basis of Student's *t* test. **(G)** U251 and U87 cells were transfected with an SFB-tagged control vector or a vector expressing SFB-PTEN for 48 h and then stimulated with EGF (100 ng/ml) for 12 h. ChIP assays with anti–β-catenin antibody and quantitative PCR analyses with primers against the promoter of *CD274* were performed. *, $P < 0.001$, on the basis of Student's *t* test. IP, immunoprecipitation; WB, Western blot.

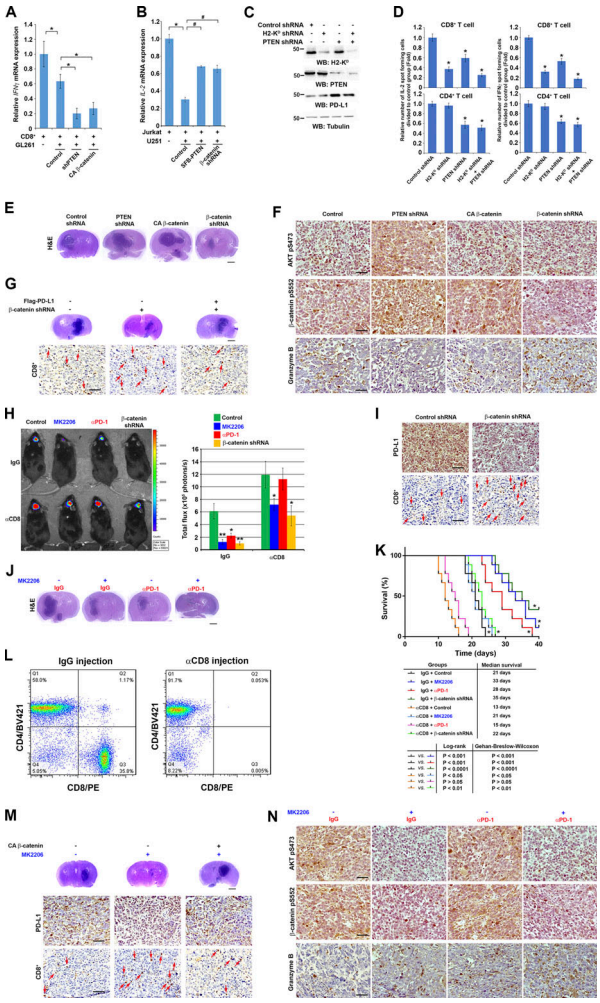

Figure S4. **β-catenin activation promotes immune evasion of tumor cells and brain tumor growth. (A)** GL261 cells with or without expressing PTEN shRNA or CA β-catenin were pretreated with Wnt3A (20 ng/ml) for 12 h to up-regulate PD-L1 expression, whereas mouse primary CD8$^+$ T cells were pre-activated for 12 h with PMA (20 ng/ml) and ionomycin (500 ng/ml). These CD8$^+$ T cells were then cultured with or without the GL261 cells for 24 h. *IFNγ* mRNA expression levels in the mouse primary CD8$^+$ T cells were measured by real-time PCR analysis. Data represent the means ± SD of three independent experiments. *, P < 0.01, on the basis of one-way ANOVA. **(B)** Jurkat T cells were preactivated for 12 h with PMA (20 ng/ml) and ionomycin (500 ng/ml) and co-cultured with or without SFB-PTEN–, β-catenin shRNA–, or control vector–expressing U251 cells that had been pretreated with Wnt3A (20 ng/ml) for 12 h to up-regulate PD-L1 expression. *IL-2* mRNA expression levels in the Jurkat T cells were measured by real-time PCR analysis 24 h after co-culture. Data represent the means ± SD of three independent experiments. *, P < 0.001; #, P < 0.01, on the basis of one-way ANOVA. **(C and D)** H2-K^D shRNA, PTEN shRNA, or a control shRNA was stably expressed in GL261 cells. **(C)** Immunoblotting analyses were performed with the indicated antibodies. **(D)** These GL261 cells were co-cultured with activated CD4$^+$ or CD8$^+$ T cells. IL-2 and IFNγ production in CD8$^+$ or CD4$^+$ T cells was determined by ELISpot analyses. Data represent the means ± SD of three independent experiments. *, P < 0.001, on the basis of one-way ANOVA. **(E)** Hematoxylin and eosin–stained coronal brain sections in Fig. 4 B show representative tumor xenografts. Scale bar, 2 mm. **(F)** The IHC staining of the mouse tumor tissues was performed with the indicated antibodies. Representative images are shown. Scale bar, 50 µm. **(G)** GL261 cells with or without expression of β-catenin shRNA or Flag–PD-L1 were intracranially injected into syngeneic C57BL/6 mice. Top panel: Hematoxylin and eosin–stained coronal brain sections show representative tumor xenografts. Scale bar, 2 mm. Bottom panel: The IHC staining of the mouse tumor tissues was performed with an anti-CD8 antibody. Representative images are shown. Scale bar, 100 µm. Red arrows point to CD8$^+$ cells. **(H, I, and K)** 10^5 CT-2A–FL cells with or without expression of β-catenin shRNA were intracranially injected into syngeneic C57BL/6 mice. The mice were treated with or without MK2206 or an anti–PD-1 antibody (as indicated in Fig. 4 F) in combination with or without an anti-CD8 antibody. Tumor growth was monitored and analyzed. **(H)** Left: Representative tumor growth is shown in vivo by bioluminescence imaging using IVIS 100 on day 15. Right: A bioluminescence imaging analysis of tumor burden was performed. *, P < 0.01; **, P < 0.001 on the basis of Student's *t* test. **(I)** The IHC staining of the mouse tumor tissues was performed with the indicated antibodies. Representative images are shown. Scale bar, 100 µm. Red arrows point to CD8$^+$ cells. **(K)** Top: The mouse survival times were recorded and visualized using Kaplan-Meier survival curves. Middle and bottom: Data represent the means ± SD of nine mice. Tables show the median survival of mice and the P values, which were calculated using the log-rank test and Gehan-Breslow-Wilcoxon test, respectively. *, P < 0.05, on the basis of Student's *t* test. **(J)** Hematoxylin and eosin–stained coronal brain sections in Fig. 4 F show representative tumor xenografts. Scale bar, 2 mm. **(L)** Quantification of CD8$^+$ T cells from spleens of the mice with IgG or an anti-CD8 antibody injection. **(M)** GL261 cells with or without expression of CA β-catenin were intracranially injected into syngeneic C57BL/6 mice. The mice were injected with or without MK2206 as described in Fig. 4 F legend. Top: Hematoxylin and eosin–stained coronal brain sections show representative tumor xenografts. Scale bar, 2 mm. Bottom: The IHC staining of the mouse tumor tissues was performed with the indicated antibodies. Representative images are shown. Scale bar, 100 µm. Red arrows point to CD8$^+$ cells. **(N)** The IHC staining of the mouse tumor tissues was performed with the indicated antibodies. Representative images are shown. Scale bar, 50 µm. WB, Western blot.

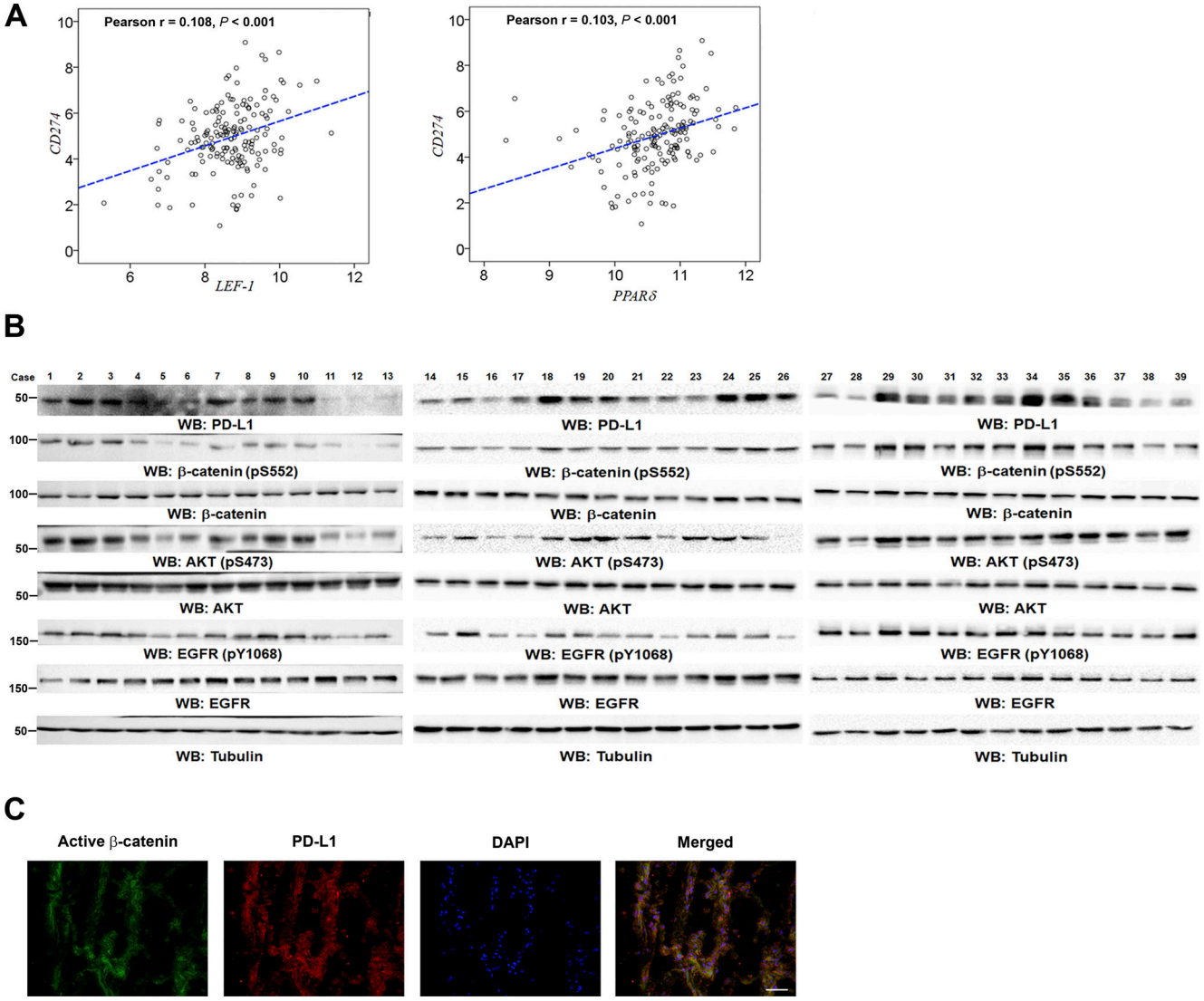

Figure S5. **PD-L1 expression is positively correlated with the levels of β-catenin S552 phosphorylation in human GBM. (A)** Correlative expression of *CD274* mRNA expression with *LEF-1* (left) and *PPARδ* (right) in the TCGA cohort of GBM (n = 145) was analyzed. Pearson r values and probabilities are presented for correlations. Gene expression values are normalized. **(B)** 39 human GBM specimens were subjected to an immunoblotting analysis with the indicated antibodies. **(C)** Immunofluorescent staining of the human GBM specimens was performed with the indicated antibodies. Scale bar, 50 µm. WB, Western blot.